CHAPTER 5
ROOF STRESS IN LONGWALL PANELS

5.1 Introduction

As analyzed in the previous chapter, the nature of the horizontal stress does have a significant influence on the stress distributions in the entry roof during the entry development. When a single longwall panel is being mined out, the entries, headgates and tailgates will be subjected to a front and a side abutment pressure caused by the longwall mining. In this case, because of the gob effects on the high horizontal stress distributions, the stresses in the immediate roof of the entries under the high horizontal stress should be different from that during the entry development. In addition, after a panel is mined out, the tailgate entries in the adjacent panel will be subjected to the side abutment pressure. In this situation, one side of the current mining panel is gob. When a high horizontal stress exists, the gob effects on the stress distributions may different from that in a single panel. Therefore, in this chapter, the stress distributions in the immediate roof of longwall entries in these two situations are analyzed.

Based on the literature review, it is found that roof failures related to a high horizontal stress mainly occur in room-and-pillar panels and during the entry development of longwall panels. In longwall panels, there is not much evidence to confirm that the high horizontal stress worsens the roof condition of entries which are in the front and side abutment zones, because in many cases the roof failure areas are in the front or side abutment zones[26, 27]. It is difficult to tell which causes the roof failure. In addition, although the numerical methods, mainly the finite element analysis, have been used to simulate the stress change with the angle, the model sizes and boundary conditions heavily influence the results. Some results seem not reasonable. Therefore, the model sizes and boundary conditions are critical for performing the numerical analysis.

Since roof failure often occurs near the two T-junctions in longwall panels, the stress distributions in the immediate roof of the entries that are in the front and side abutment zones (around the two T-junctions) are studied. Based on the previous analysis, it is found that the overburden depth and the stress ratio of the maximum to the minimum horizontal stress are not important factors that influences the stress distributions in the immediate roof. Therefore, in this study, the overburden depth is fixed, 800 psi, and the ratio is 2.0. In addition, since the roof failure mainly occurs in the weak roof, a weak roof is used in the finite element analysis. Moreover, based on the previous stress analysis it is found that the stress angle between the mining direction and the maximum horizontal stress is the most important factor affecting the stress distributions in the immediate roof of longwall entries. Therefore, the stress distributions in the weak roof will be studied when the angle ranges from 0^0 to 90^0, namely, the influence of the stress angle on the stress in the longwall entry roof is analyzed.

In this study, two situations are involved. First, the stresses in the entry roof in a single longwall panel are analyzed. Then the stresses in the entries of the adjacent panel are studied, after a panel is mined out. Since roof failure often occurs in the abutment zones, the stress distributions in the zones without horizontal stress are studied first. Then the stress distributions with horizontal stress are analyzed. Through the comparisons between these two situations, the horizontal stress influence on the roof stress can be found.

5.2 Finite Element Models

In this study, the basic models are shown in Figs. 5-1 and 5-2. The model length and width range from 2,000 ft to 3,000 ft. The angle between the mining direction and the maximum horizontal stress is 0^0, 15^0, 30^0, 45^0, 60^0, 75^0, and 90^0, respectively. The mining face is 800 ft wide and the mining height is 7 ft. The chain pillar is 80 ft wide and 100 ft long. The entry width is 18 ft. The gob length is 1,200 ft. As discussed in Chapter 4, the overburden depth is not an important factor. Therefore, in the following studies, the overburden depth is 800 ft.

In each entry, the Von-Mises stress, maximum and minimum principal stresses along three lines, line L, line C, and line R in Figs. 5-1 and 5-2 in the section of interest (near the T-junctions) will be analyzed. Line L and line R are along the rib sides and line C is in the center of the entry.

The overburden roof strata are disturbed in order of severity from the immediate roof toward the surface, when a longwall panel is excavated. Generally, the disturbed strata can be divided into 3 zones: the caved zone, the fractured zone, and the continuous zone. Since the strata in the continuous zone deformation zone have no major cracks, it is reasonable to assume the vertical stress is uniformed in this zone. Therefore, the model height should at least be equal to the height of the caved and fractured zones. Usually, the height of these two zones is about 30~50 times of mining height, as shown in Fig. 5-3. Since the mining height in this study is 7 ft, the model height should be 210~350 ft. In this study, the roof thickness in the model is 350 ft and the floor thickness is 50 ft. Therefore, the total height of the model is 407 ft. The geological conditions are the same as those in the previous chapter, as listed in Table 4-1. In this study, only the weak roof is involved. The models and meshes are shown in Fig. 5-4. The minimum element size is 2x2x3 ft. The total number of the elements in a model is about 35,000 to 55,000.

In the disturbed strata, the rock properties have changed. Usually, their Young's modulus and weights reduce and the Poisson's ratios increase. The gob in the models has a significant effect on the stress distributions in the entry roof. Based on the previous studies and the surface subsidence data, the gob effect can be considered by systemtically reducing the gob material properties, such as unit weight, Young's modulus, and Poisson's ratios. The reduction factors used in this study are list in table 5-1. The gob is divided into three zones, loose zone, packed zone, and well packed zone.

Table 5-1 Reduction Factors for Gob Materials

Gob Zone	**Reduction Factor**		
	Density	**Young's Modulus**	**Poisson's Ratio**
loose	2/3	1/100	1/10
packed	1/4	1/50	1/5
well packed	1/5	1/10	1/3

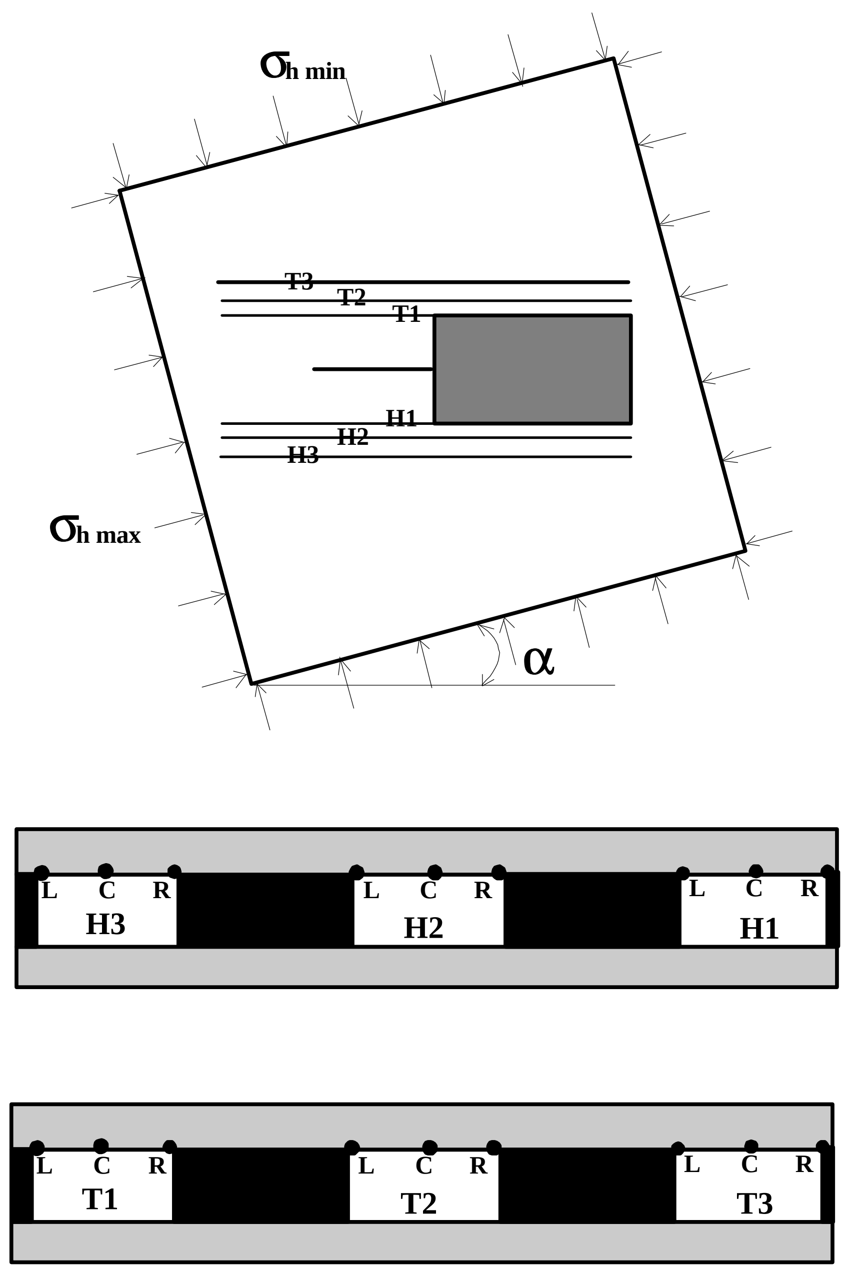

Fig. 5-1 Plan View of Basic Model for Single Panel and Locations of Lines
H – Headgates; T – Tailgates

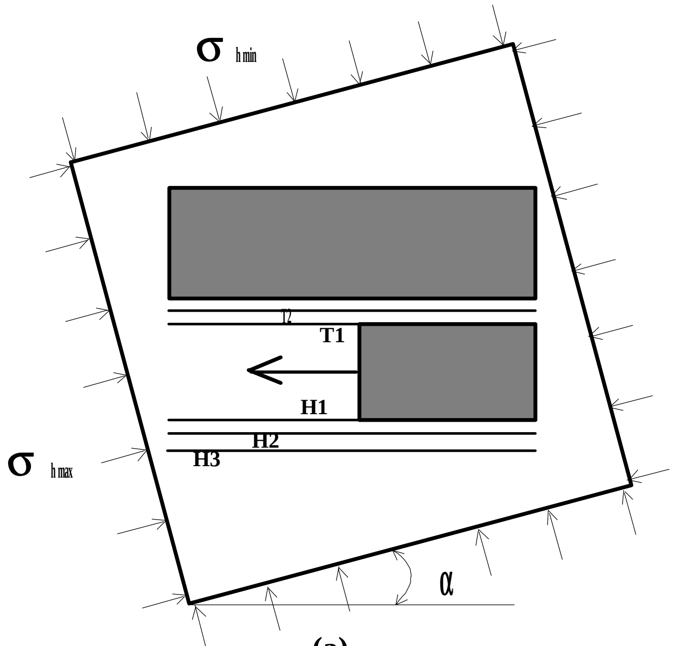

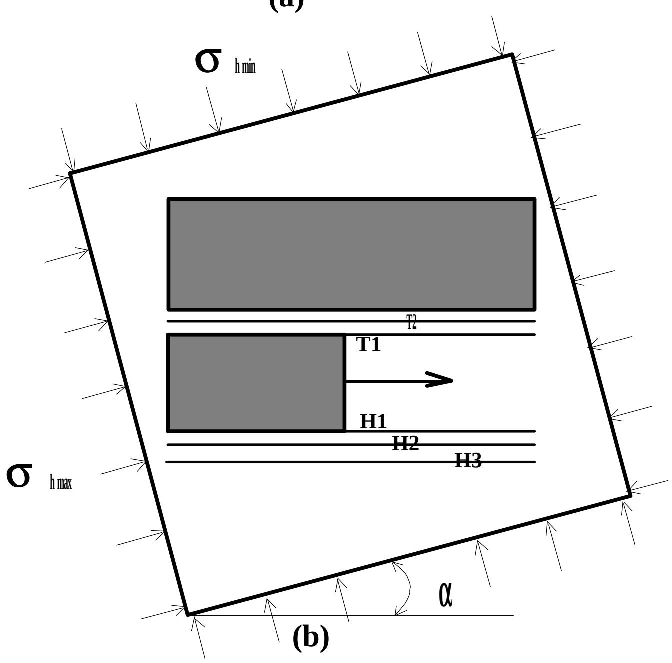

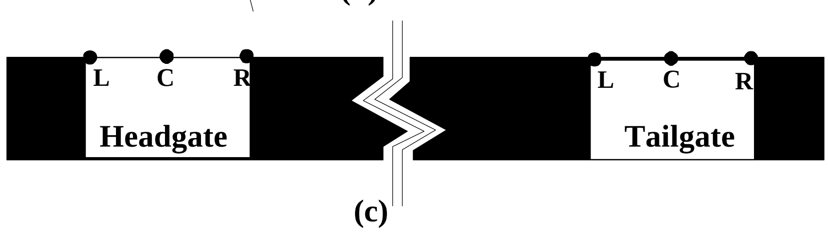

Fig. 5-2 Plan View of Basic Model for Multiple Panels and Locations of Lines σ_{hmax} from Solid coal Side; (b) σ_{hmin} from Gob Side (c) Locations of lines L, C, and R in Entries

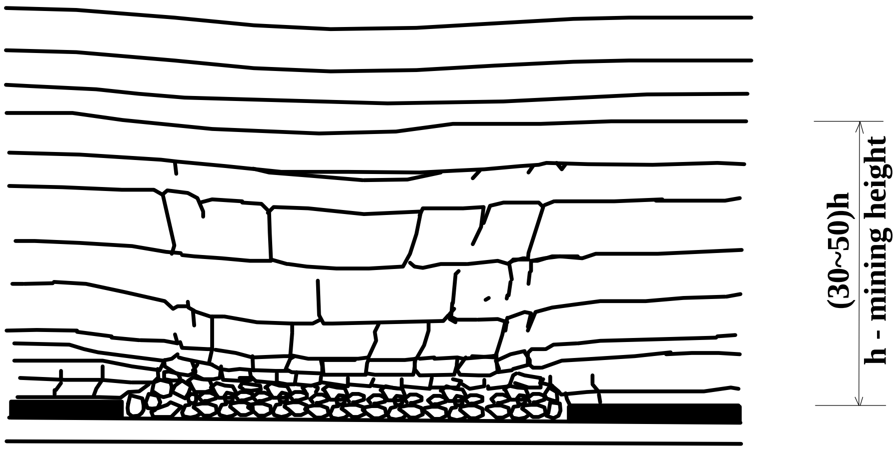

(a) Overburden Movement

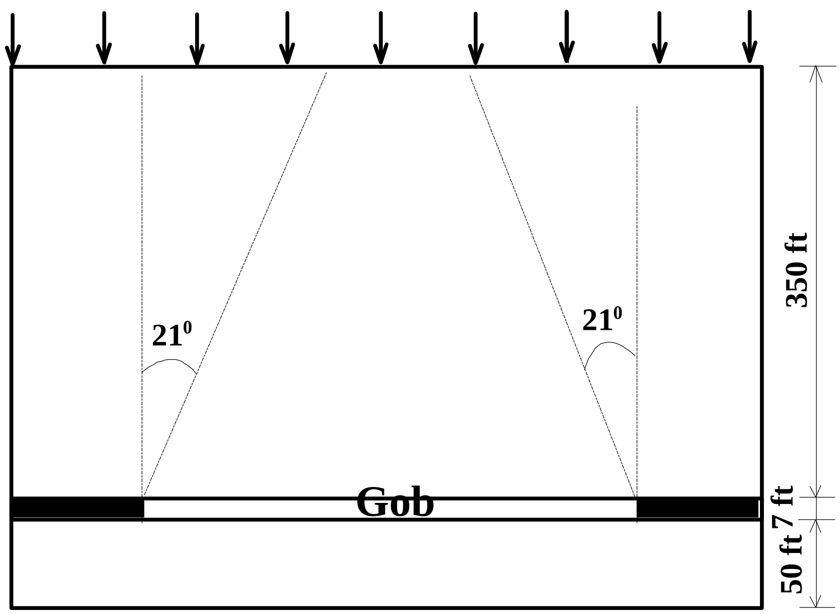

(b) Model Height

Fig. 5-3 Determination of Model Height

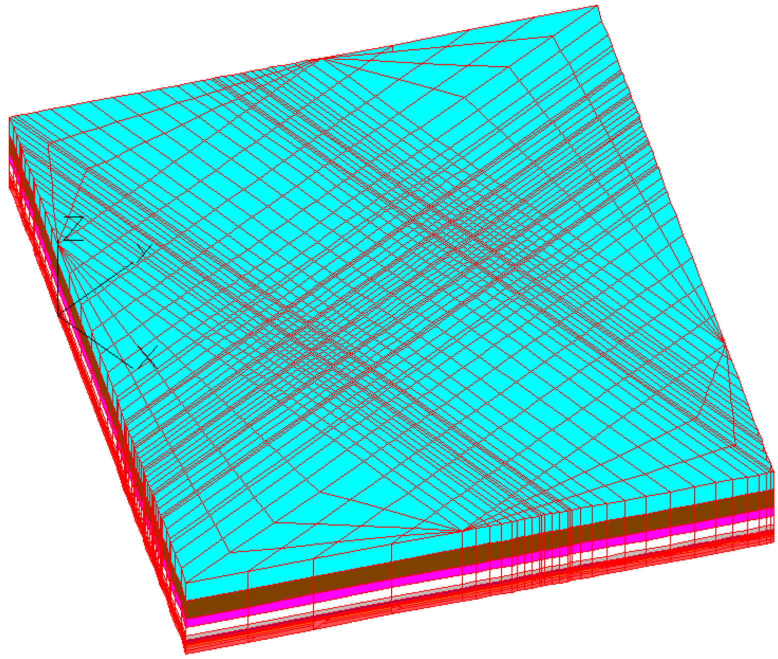

(a) Single Panel

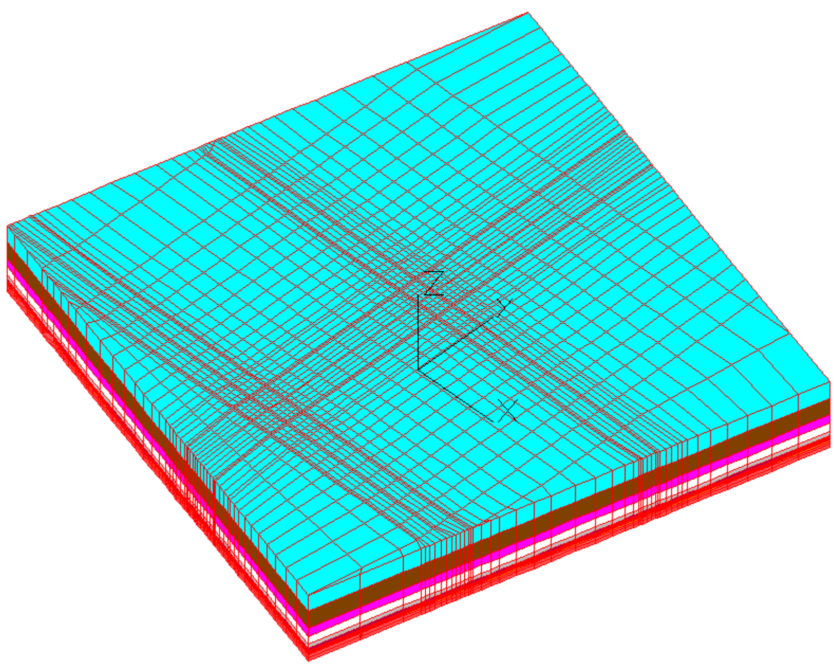

(b) Multiple Panels

Fig. 5-4 Models and Meshes for Longwall Panels

5.3 Stress in Entry Roof in a Single Panel

5.3.1 Stress Distributions without Horizontal Stress

The stress distributions at the roof line level near the T-junctions in a single longwall panel are analyzed here. Since the stresses in the headgates are the same as those in the tailgates in this case, only the stresses in the headgates are studied.

In headgate 1 (H1 in Fig. 5-1), the section near the T-junction is subjected to the front abutment pressure. The stresses at the roof line level are shown in Fig. 5-5. It shows the Von-Mises, the maximum and minimum principal stresses along the five lines, numbered L1 ~L5. The locations of these lines are shown in Fig. 5-5(a). The distance between line L1 (or L5) to line L2 (L4) is about 1.5 ft. Line L3 is in the center of the roof.

The Von-Mises stresses along lines L1 ~ L5 are shown in Fig. 5-5(a). It indicates that the Von-Mises stress is concentrated at the pillar rib side. Because of the influence of the crosscuts, the stress along line L1 is slightly larger than that along line L5. Without such influence, the stress along line L5 is slightly larger than that along line L1. Fig. 5-5(a) also indicates that the major influence zone of the front abutment pressure is about 50 ft. At the center of the entry, the Von-Mises stress is smaller.

The minimum principal stress is shown in Fig. 5-5(b). Along lines L2~L4, the stress is less than zero, namely the roof along these lines are in tension. Usually, the tensile stress at the center of the roof is larger. But in the front abutment zone, the tensile stress increases, especially along lines L2 and L4. At the rib sides, no tensile stress occurs.

The maximum principal stress is distributed in the similar way as the Von-Mises stress, as shown in Fig. 5-5(c). The maximum principal stresses along the rib sides (L1 and L5) are larger. At the center of the roof, the maximum principal stress is near zero. This figure also indicates that the major influence zone of the front abutment pressure is about 50 ft.

In headgate 2 (H2 in Fig. 5-1), the stresses at the roof line level are shown in Fig. 5-6. The Von-Mises stress is shown in Fig. 5-6(a). The Von-Mises stress along line L1 is slightly larger than that along line L5 in the gob side. Generally the stress at the rib side near headgate 1 is smaller than that at the other side in the front and side abutment zones. But they are the same outby the front abutment zone. At the center, the stress is smaller. The Von-Mises stress in headgate 2 is smaller than that in headgate 1.

The minimum principal stress in headgate 2 is similar to that in headgate 1, as shown in Fig. 5-6(b). But the difference between the stresses along the two rib side is larger than that in headgate 1. Except those at the rib sides, the roof is in tension (along lines L2~L4).

The maximum principal stress is shown in Fig. 5-6(c). In the abutment zones, the maximum principal stress along line L1 is larger than that along line L5. At the center of the roof, the stress is very small.

In headgate 2, the Von-Mises stress and the maximum and the minimum principal stresses along line L1 (Fig. 5-6) inby the mining face (within 0 ~ -120 ft) is larger because of the side abutment pressure. The stresses in this section are larger than that in the front abutment zone.

In headgate 3 (H3 in Fig. 5-1), the Von-Mises, minimum and maximum principal stresses distributions at the roof line level are shown in Fig. 5-7. It indicates that the abutment pressure has little influence on headgate 3. The stresses are the smallest among the three headgates.

Since the overburden moves toward to the gob, the stress distributions in headgates 1, 2, and 3 are not symmetric. Generally, the Von-Mises Stress and the minimum and maximum principal stresses along line L1 are slightly larger than those along line L5. But the difference between them is very small. In addition, the Von-Mises stress and the maximum principal stress are concentrated along the entry rib sides. This indicates that the possibility of cutter roof still exists in longwall entries without horizontal stress.

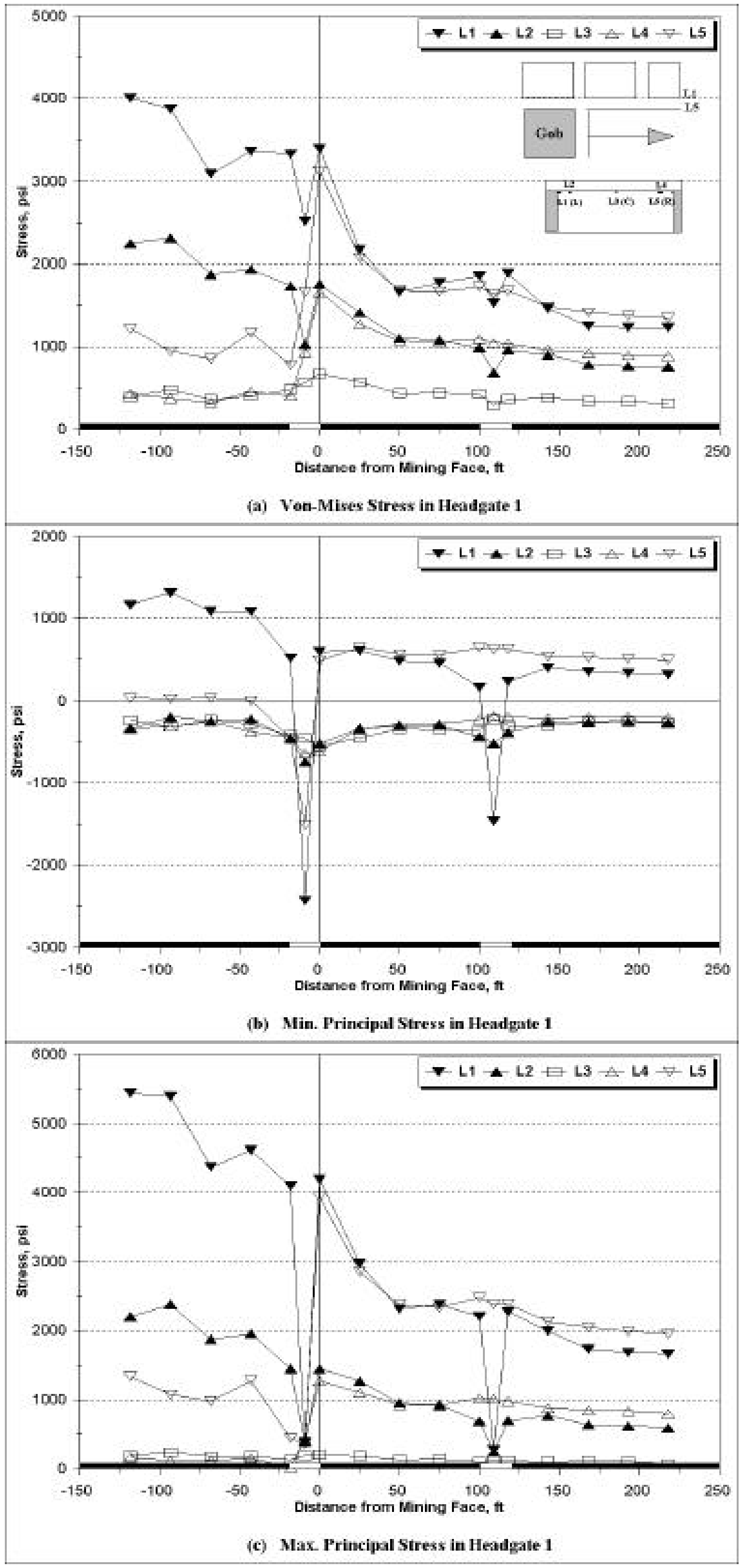

Fig. 5-5 Stress Distributions at Roof Line Level in Headgate 1 (in single panel without horizontal stress)

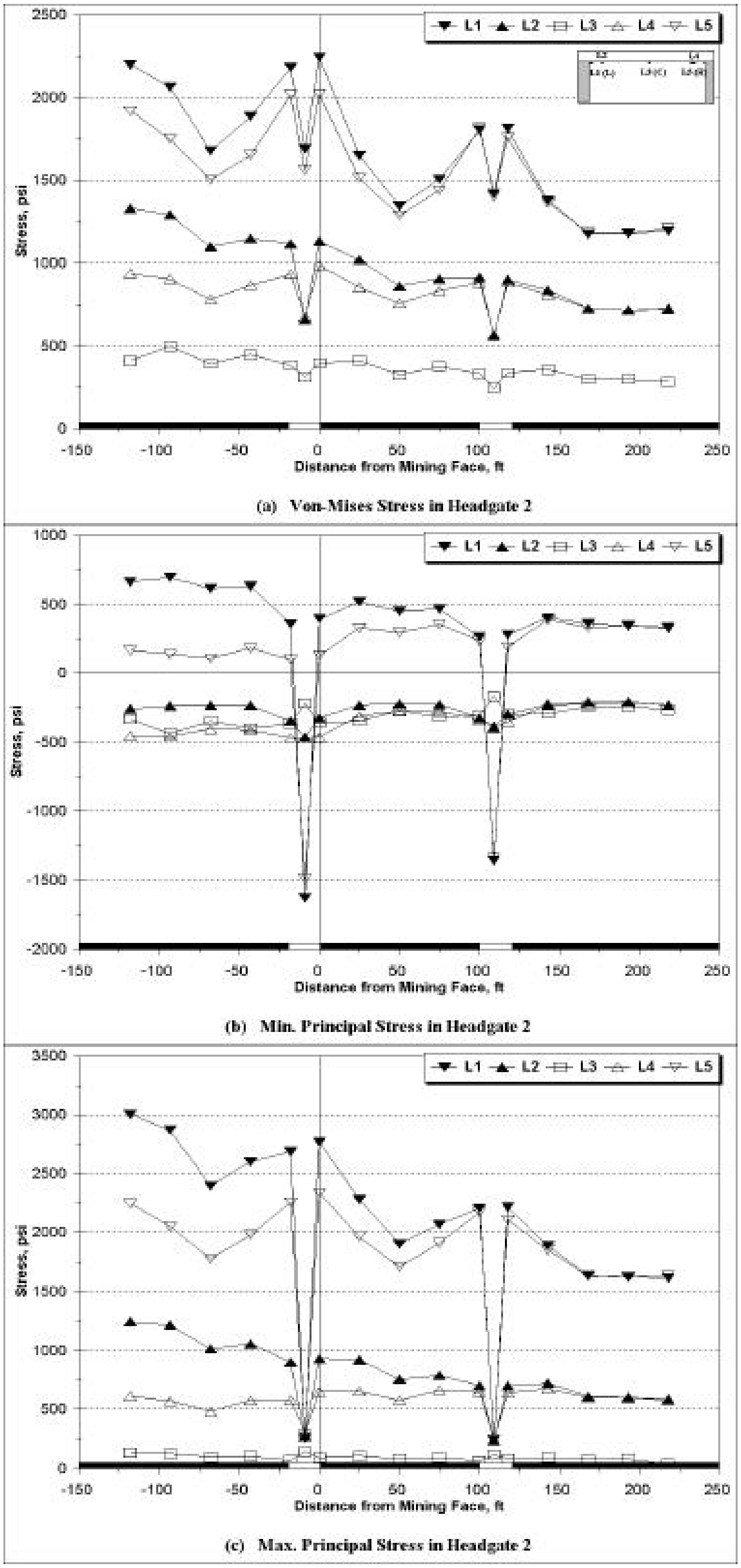

Fig. 5-6 Stress Distributions at Roof Line Level in Headgate 2 (in single panel without horizontal stress)

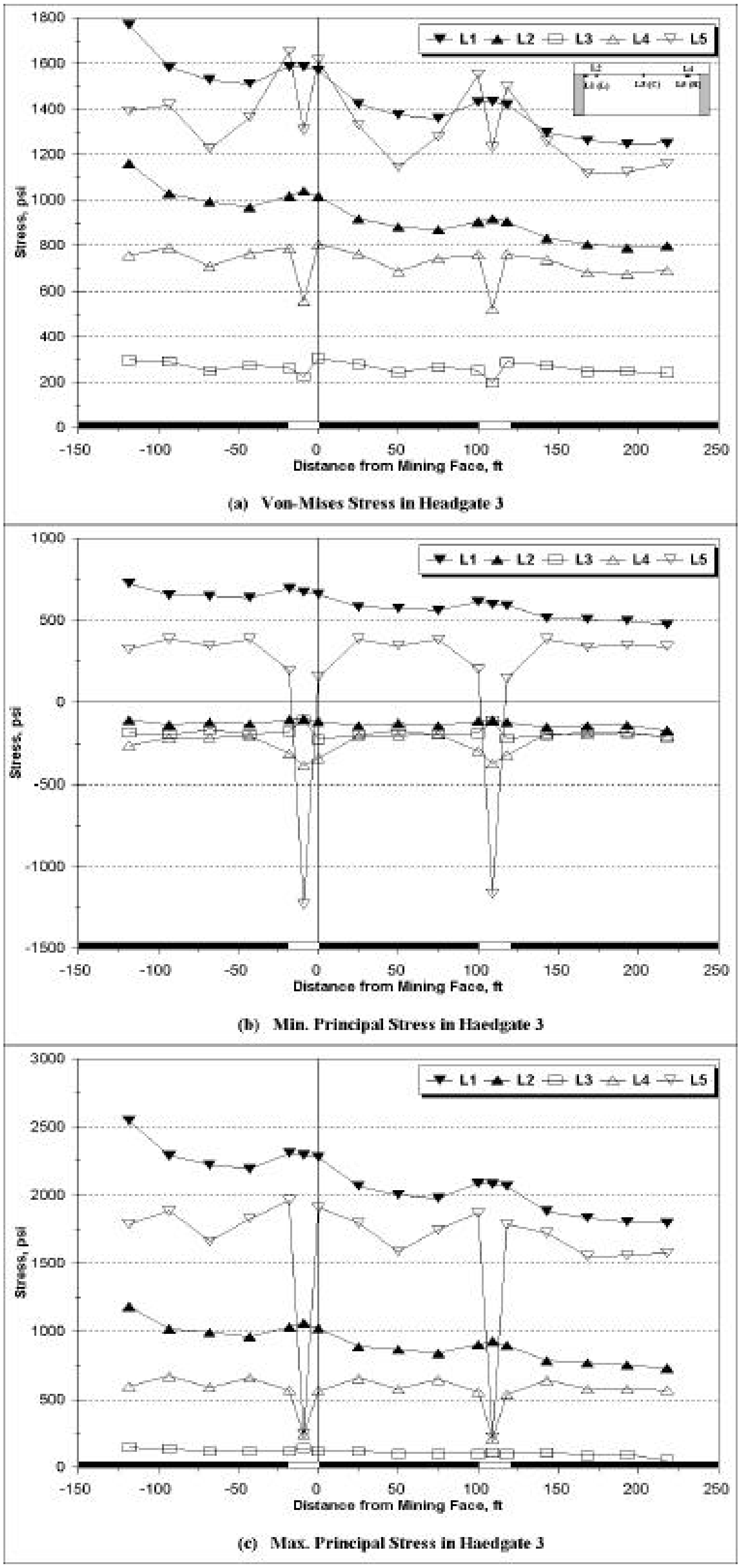

(a) Von-Mises Stress in Headgate 3

(b) Min. Principal Stress in Haedgate 3

(c) Max. Principal Stress in Haedgate 3

Fig. 5-7 Stress Distributions at Roof Line Level of Headgate 3 (in single panel without horizontal stress)

5.3.2 Stress Distributions with Horizontal Stress

High horizontal stress is a significant factor in ground control in longwall mines. It can be destructive to the entries near the T-junctions in longall retreat. In the following section, the Von-Mises stress and the maximum and minimum principal stresses at the roof line level near the T-junctions will be analyzed. Based on the above analysis, the stress in Headgate 3 and Tailgate 3 is the smallest in the whole entry system. Therefore, the stresses in the roof of headgates 1 and 2 and tailgates 1 and 2 are analyzed in the following. In addition, since the stresses in the roof near the T-junctions are very large, emphasis is placed on the stresses along lines L, C, and R in headgate 1 and tailgate 1 (see Fig. 5-1).

<u>Stresses in Headgate 1</u>

Near the T-junction in headgate 1, the entry is subjected to the large front abutment pressure. Roof failure often occurs in this area. Under the high horizontal stress, the stress is affected by the angle between the maximum horizontal stress and the mining direction. In this study, the maximum horizontal stress is from the headgate side.

a. Von-Mises Stress

The Von-Mises stress at the roof line level near the T-junction is shown in Fig. 5-8. It shows the stress distribution along the three lines near the T-junction, line L, line C, and line R. Along line L, the Von-Mises stress with the horizontal stress is larger than that without horizontal stress in the front abutment zone, as shown in Fig. 5-8(a). However, inby the longwall face, the stress with the horizontal stress is less than that without the horizontal stress, except at a few points. At the center of the entry, the Von-Mises Stress with the horizontal stress is significantly larger than that without the horizontal stress, as shown in Fig. 5-8(b). Along the other rib side (line R), the Von-Mises stress with the horizontal stress is larger than that without the horizontal stress, as shown in Fig. 5-8(c). Generally, the Von-Mises stress increases with the angle. In the front abutment zone, the stresses are concentrated at the rib sides and the Von-Mises stress along the lonwall face side is larger than that along the pillar side.

At the T-junction, the Von-Mises stress distributions are shown in Fig. 5-9. At point P1, the Von-Mises stress increases with the angle from 0^0 to 75^0, and then decreases slightly from 75^0 to 90^0. At point P3, the stress increases with the angel from 0^0 to 60^0, and then decreases 60^0 to 90^0. At point P2, the angle influence is not significant. At the intersection between the crosscut and headgate 1, the Von-Mises stress is larger. At point P4, the stress is larger than that at point P1, except when the angle is 90^0. At point P1, the stress reaches the maximum when the angle is about 75^0. At point P5, the stress increases with the angle from 0^0 to 60^0, and then decreases from 60^0 to 90^0. Around the T-junction, the stress at this point is the maximum. Because of the gob effects, the stresses at points P6 and P7 generally decrease with the angle. Along the rib side from P5 to P7, the Von-Mises stress with the horizontal stress is less than that without horizontal stress, as shown in Fig. 5-8(a). This indicates stress relieves at this area because of the gob effects.

b. Maximum Principal Stress

The maximum principal stress at the roof line level is shown in Fig. 5-10. Generally, the stress outby the face is larger with the horizontal stress than that without horizontal stress. The distribution of the maximum principal stress is similar to the Von-Mises stress distribution. Along line L, the maximum principal stress increases with the angle from 0^0 to 60^0, and then decreases slightly from 60^0 to 90^0. But inby the longwall face, the stress with horizontal stress is less than that without horizontal stress, as shown in Fig. 5-10(a).

At the center of the entry, the maximum principal stress also increases with the angle from 0^0 to 60^0, and then decreases slightly from 60^0 to 90^0, as shown in Fig. 5-10(b). Without horizontal stress, the stress at the center is very small. Under the horizontal stress, the stress is much larger.

The maximum principal stress at the other rib side is shown in Fig. 5-10(c). In the front abutment zone, the stress with horizontal stress is larger than that without the horizontal stress, and increases with the angle from 0^0 to 60^0, and then decreases from 60^0 to 90^0.

Near the T-junction, the maximum principal stress at points P1~P7 is shown in Fig. 5-11. The stresses at points P1 and P3 increase with the angle from 0^0 to 60^0, and then decrease slightly from 60^0 to 90^0. However, the stress at point P3 is larger than that at point P1. At point P2, the stress changes slightly with the angle. At point P5, the stress is the largest.

c. Minimum Principal Stress

The minimum principal stress at the roof line level in headgate 1 is shown in Figs. 5-12 and 5-13. Under the horizontal stress, the minimum principal stress in the roof is larger than that without the horizontal stress. At points P1 and P3, the stress increases with the angle from 0^0 to 60^0, and then decreases slightly from 60^0 to 90^0. However, the angle influence on the minimum principal stress is not as significant as that on the Von-Mises stress and the maximum principal stress. Under the combined influence of the front and side abutment pressures, tensile stress may occur in the T-junction. For example, the tensile stress may occur at points P2 and P4.

In headgate 1, the stresses including the Von-Mises stress and the maximum and minimum principal stress, are affected by the angle between the mining direction and the maximum horizontal stress. Under the horizontal stress, the stresses at the T-junction are larger than those without horizontal stress. They increase with the angle. When the angle is about 60^0 ~ 75^0, the stresses reach the maximum, i.e. the T-junction is subjected to the worst condition.

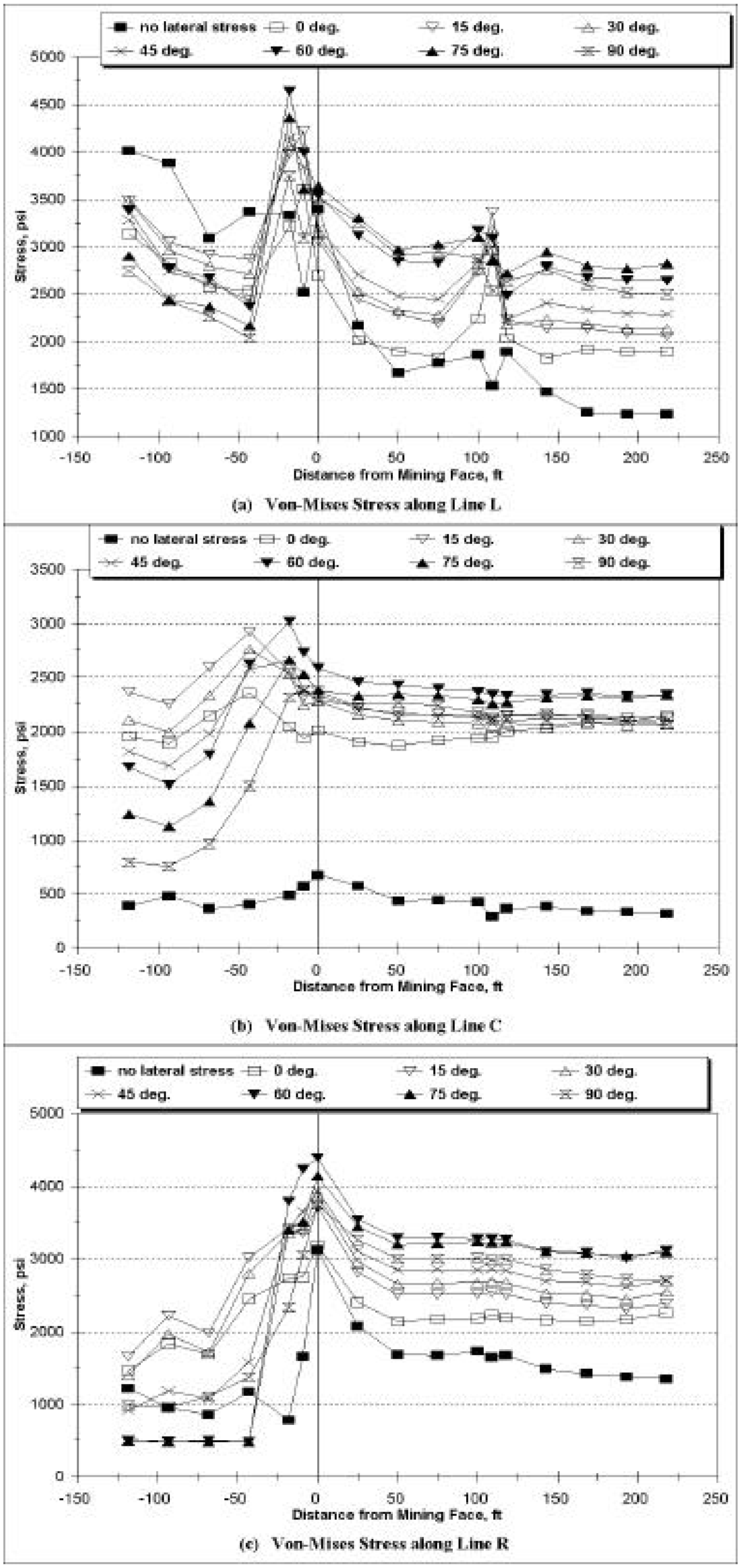

Fig. 5-8 Von-Mises Stress in Headgate 1 (in single panel)

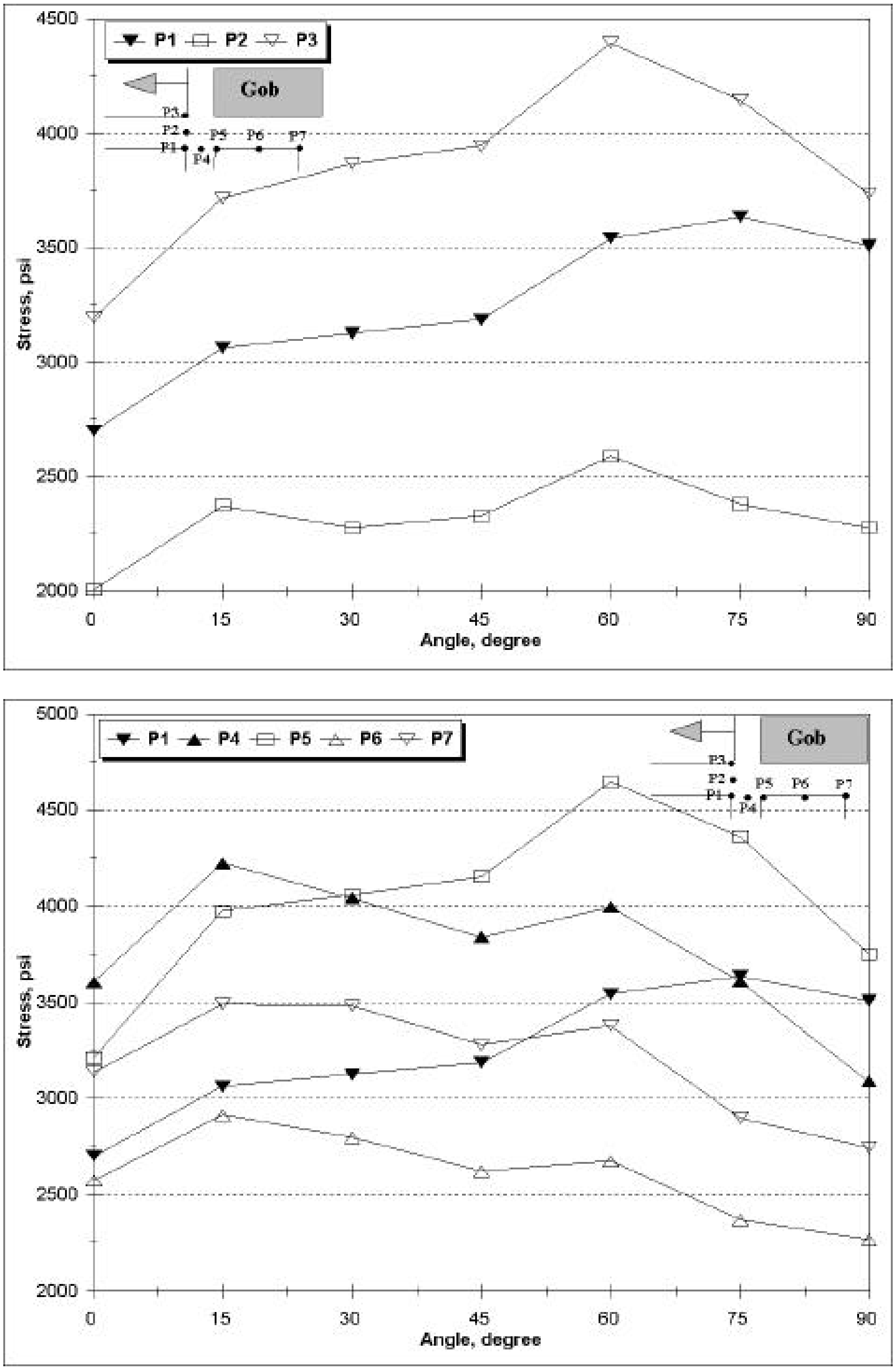

Fig. 5-9 Von-Mises Stress at the Some Points in Headgate 1 (in single panel)

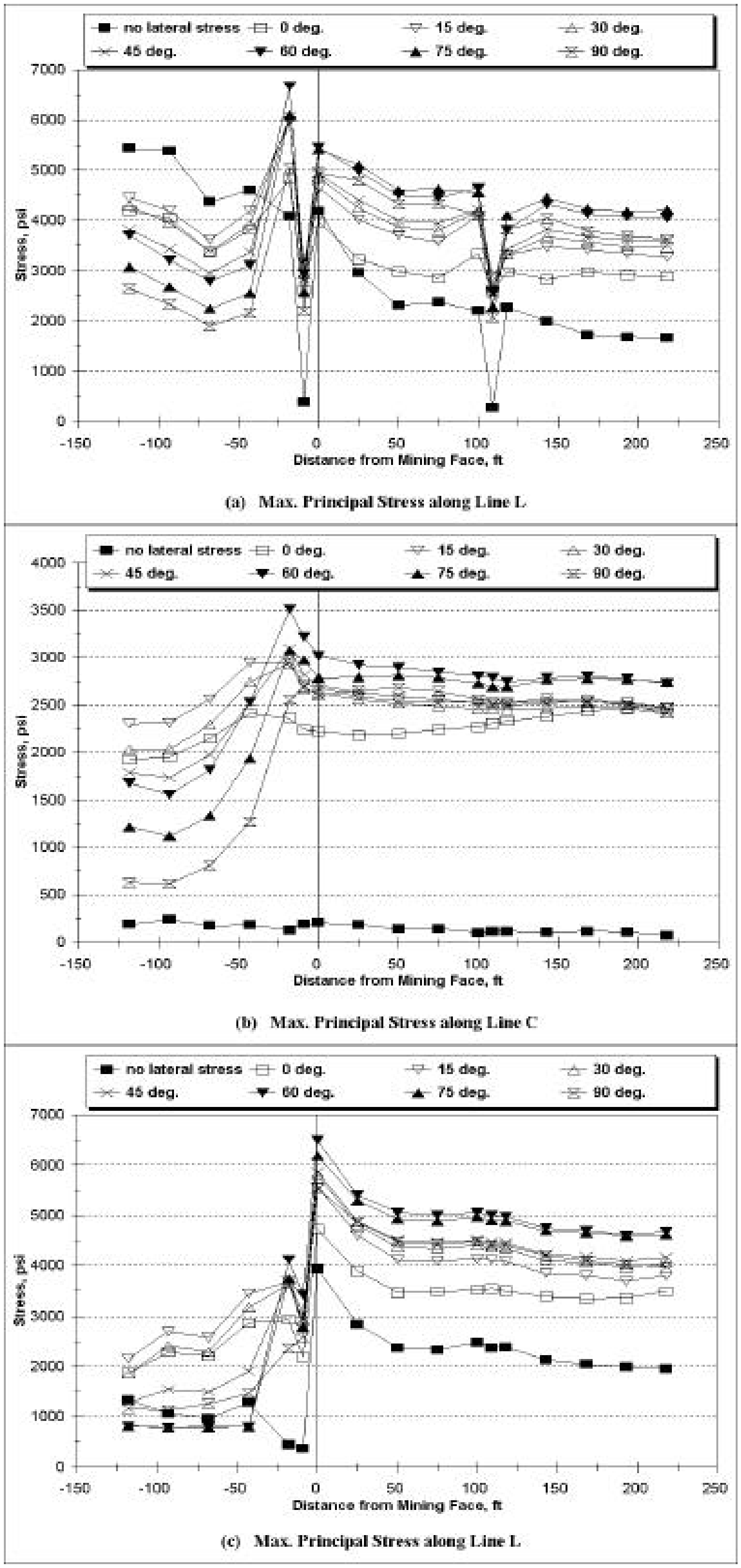

Fig. 5-10 Max. Principal Stress in Headgate 1 (in single panel)

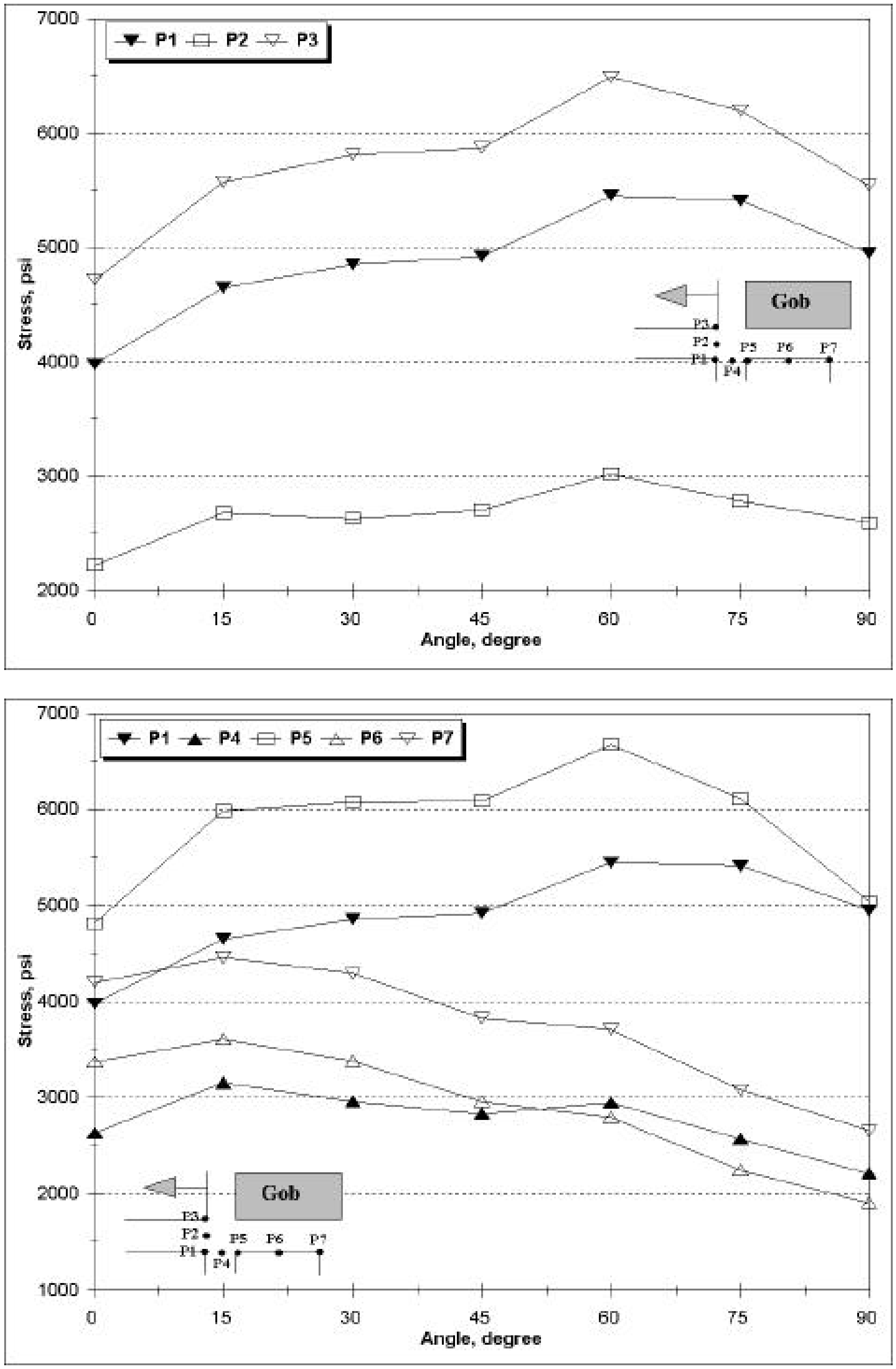

Fig. 5-11 Max. Principal Stress at the Specified Points in Headgate 1 (in single panel)

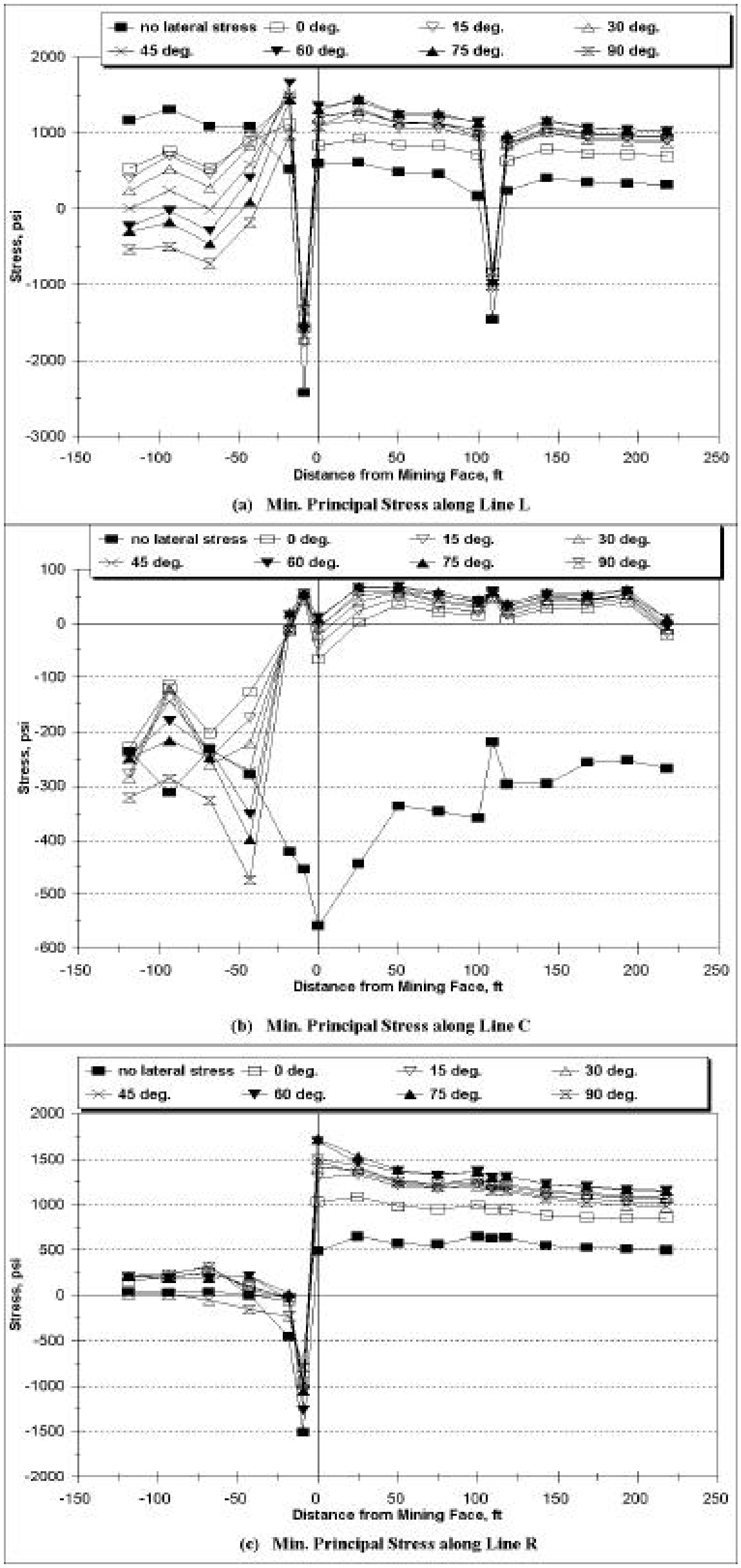

(a) Min. Principal Stress along Line L

(b) Min. Principal Stress along Line C

(c) Min. Principal Stress along Line R

Fig. 5-12 Min. Principal Stress in Headgate 1 (in single panel)

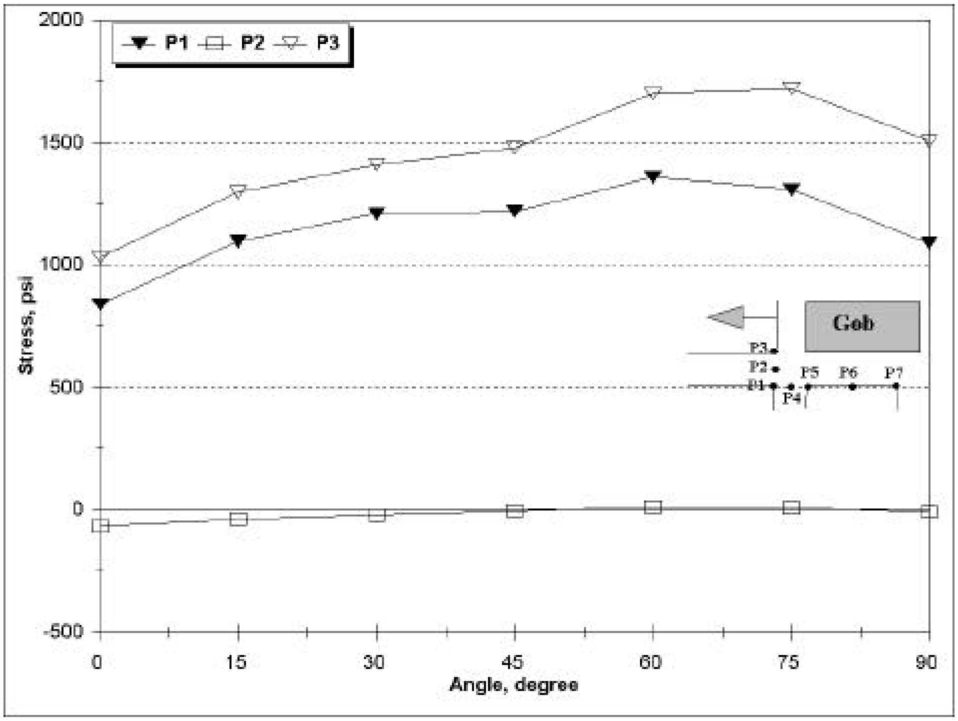

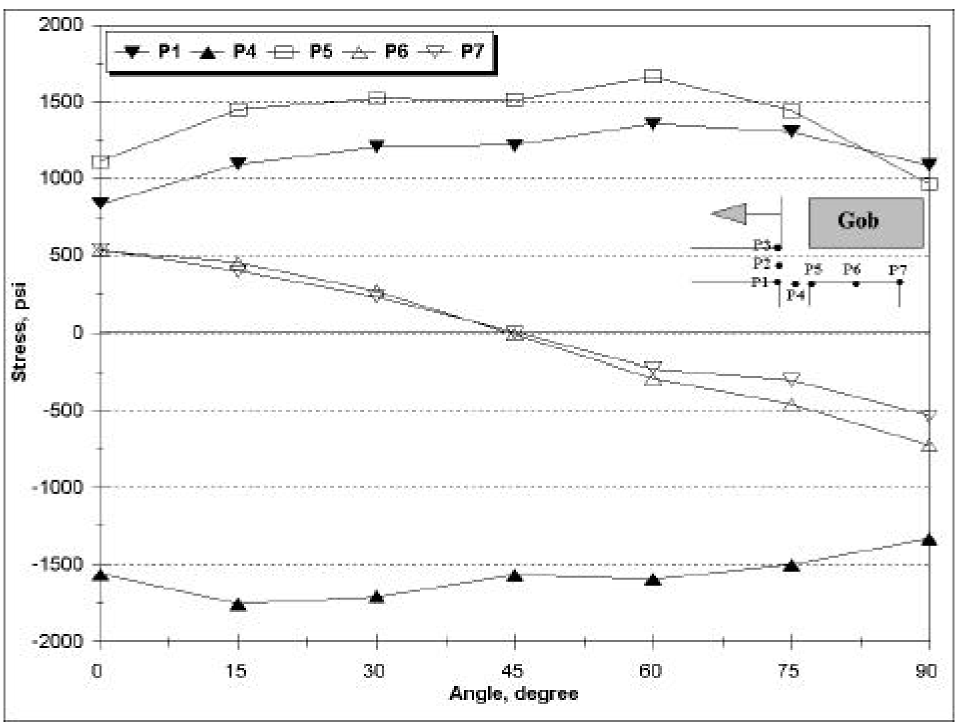

Fig. 5-13 Min. Principal Stress at the Some Points in Headgate 1 (in single panel)

Stresses in Tailgate 1

In tailgate 1, the stress in the entry roof near the T-junction is usually larger than that in the other sections. The Von-Mises stress and the maximum and minimum principals stresses at the roof line level in this section will be analyzed in the following.

a. Von-Mises Stress

The Von-Mises stress at the roof line level is shown in Fig. 5-14. The stress is concentrated at the two rib sides. It changes with the angle between the mining direction and the maximum horizontal stress. Along line L, the Von-Mises stress increases with the angle from 0^0 to 60^0, and then decreases from 60^0 to 90^0, as shown in Fig. 5-14(a). At the center of the roof, the stress increases with the angle from 0^0 to 90^0, as shown in Fig. 5-14(b). Along line R, the stress increases with the angle from 0^0 to 90^0, as shown in Fig. 5-14(c). The stress distributions in tailgate 1 is similar to that in headgate 1. The stress in the immediate roof with the horizontal stress is larger than that without the horizontal stress.

At the T-junction, the Von-Mises stress at various points is shown in Fig. 5-15. At point P1, the stress increases with the angle from 0^0 to 75^0, and then stays nearly unchanged. At point P3, the stress increases with the angle from 0^0 to 60^0, and then decreases slightly from 60^0 to 90^0. At point P2, the angle influence is not significant. At point P4, which is at the center of the intersection between tailgate 1 and the crosscut, the Von-Mises stress reaches the maximum when the angle is about 15^0. At point P5, the stress is larger than that at point P1. When the angle is about 90^0, the stress at point P5 reaches the maximum, being the largest of all.

b. Maximum Principal Stress

The maximum principal stress at the T-junction of tailgate 1 is similar to the Von-Mises stress, as shown in Fig. 5-16. Big stress concentration occurs at the two rib sides. It increases with the angle from 0^0 to 75^0, and then decreases slightly from 75^0 to 90^0.

The maximum principal stress for various the points is shown in Fig. 5-17. The larger stress occurs at points P1, P3, and P5. But, the stress at point P1 is less than that at point P3.

c. Minimum Principal Stress

The minimum principal stress in tailgate 1 is shown in Figs. 5-18 and 5-19. Under the horizontal stress, the minimum principal stress in the immediate roof of tailgate 1 is larger than that without the horizontal stress. Usually, the minimum principal stress increases with the angle. However, the angle influence on the stress is not as significant as that on the Von-Mises stress and the maximum horizontal stress.

In tailgate 1, the Von-Mises stress and the maximum and minimum principal stresses increases with the angle between the mining direction and the maximum horizontal stress. When the angle is about $60^0 \sim 75^0$, tailgate 1 is in the worst condition.

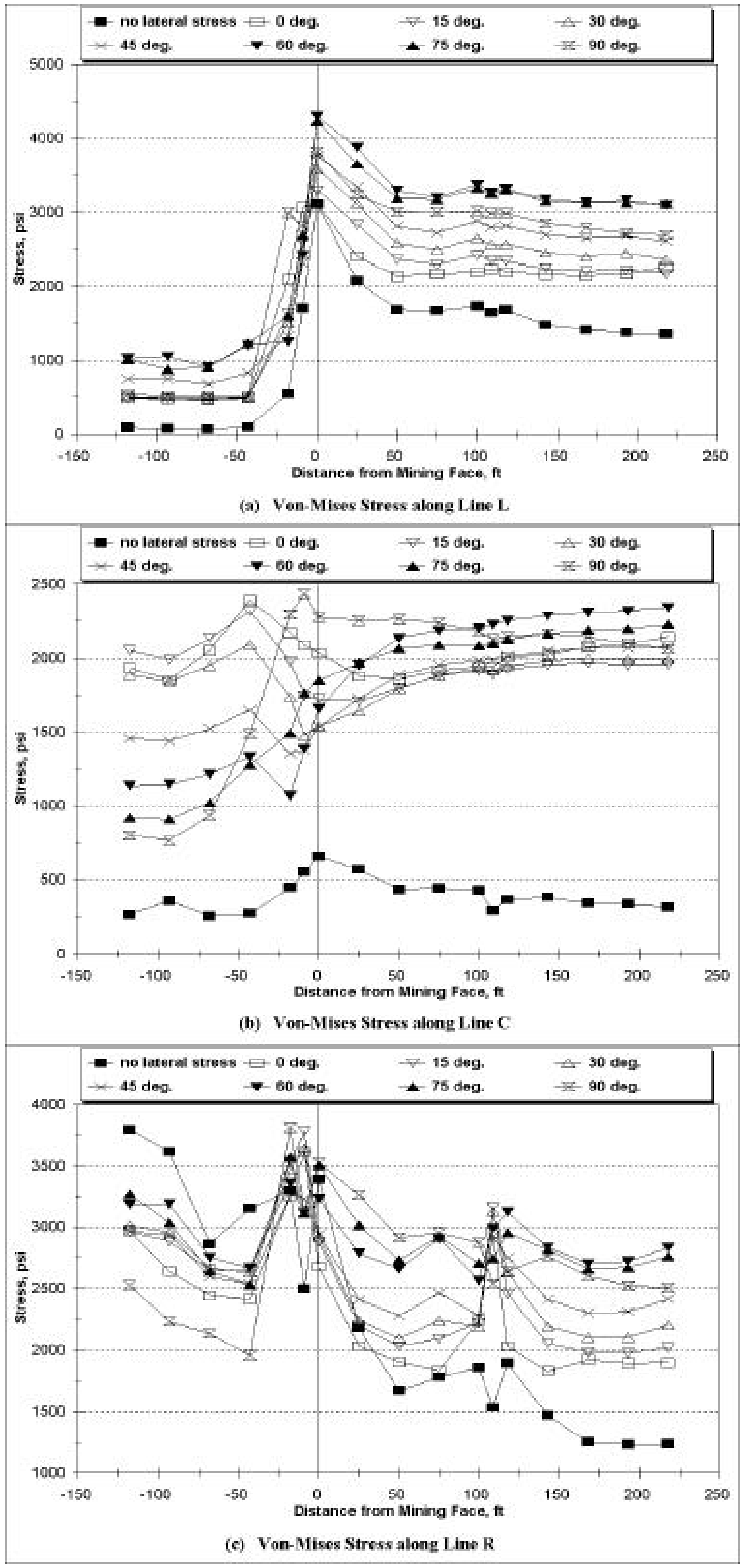

Fig. 5-14 Von-Mises Stress in Tailgate 1 (in single panel)

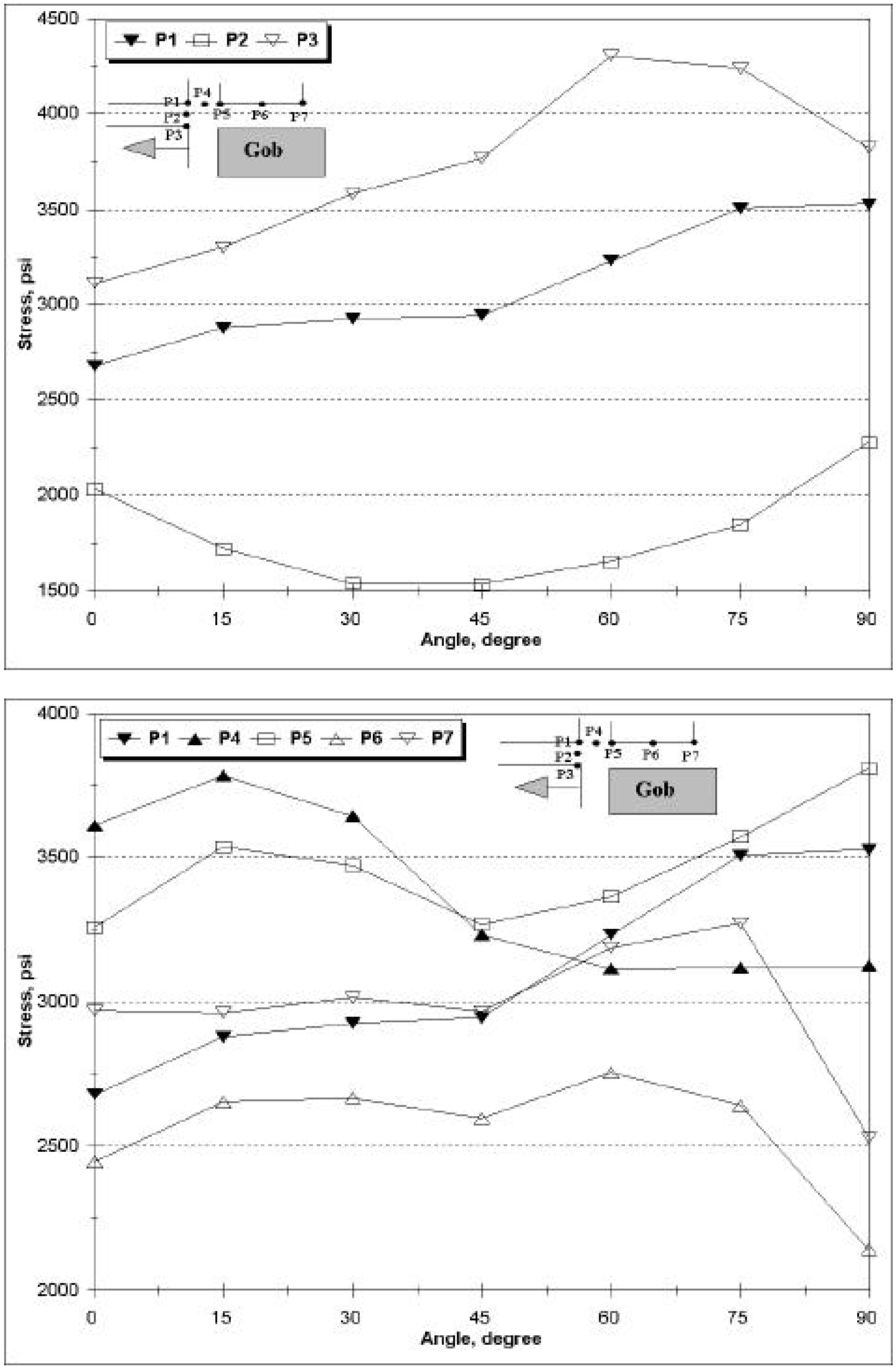

Fig. 5-15 Von-Mises Stress at the Some Points in Tailgate 1 (in single panel)

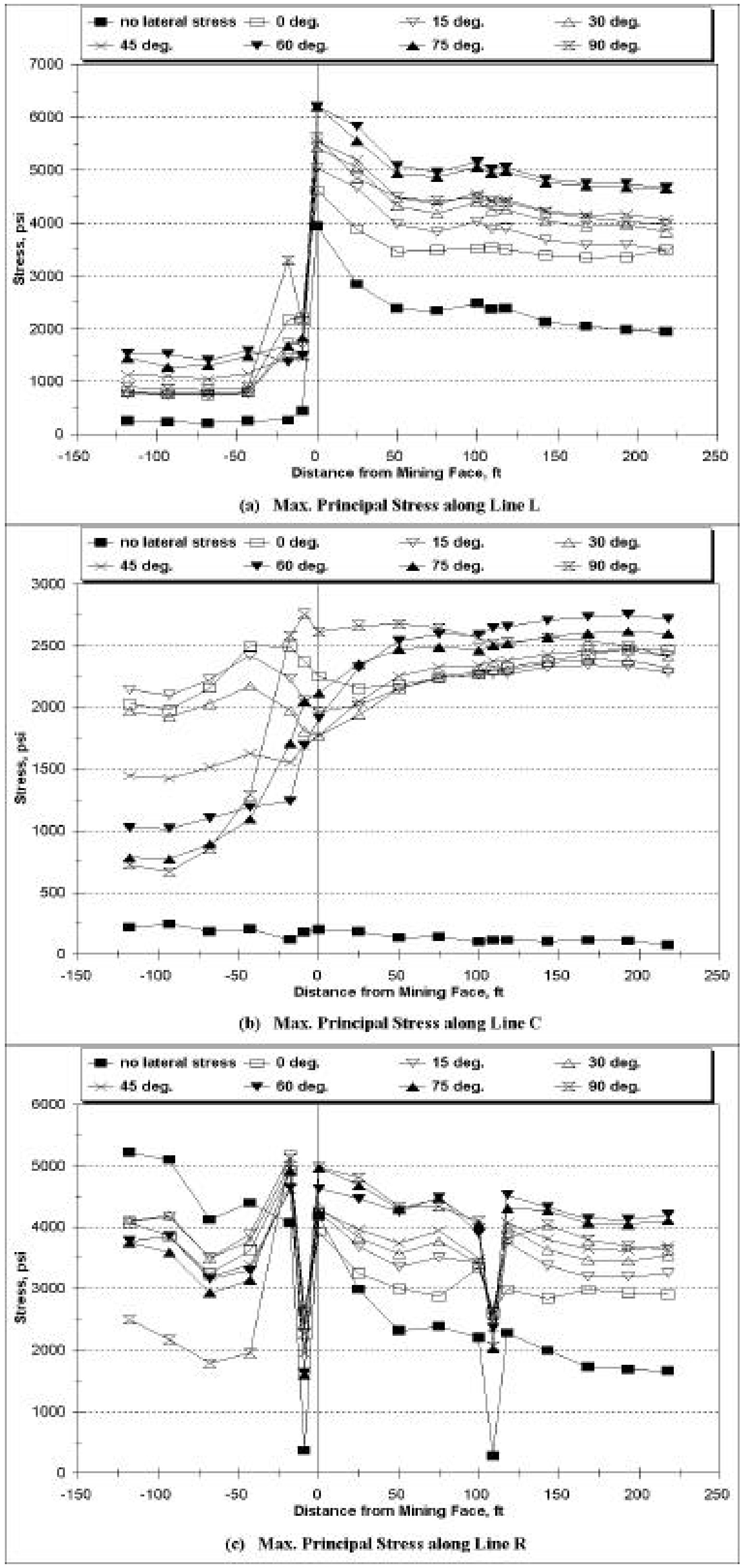

Fig. 5-16 Max. Principal Stress in Tailgate 1 (in single panel)

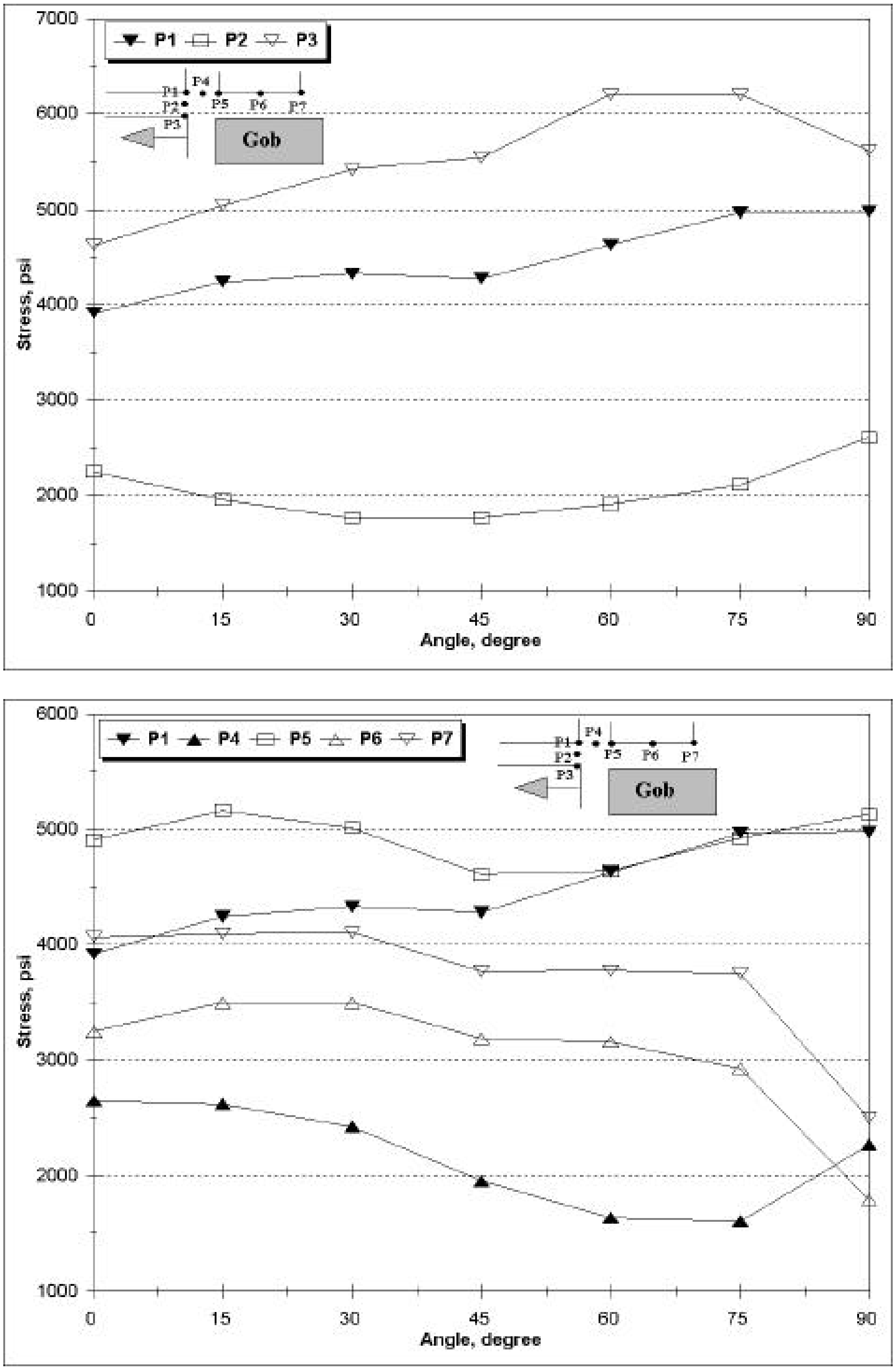

Fig. 5-17 Max. Principal Stress at the Some Points in Tailgate 1 (in single panel)

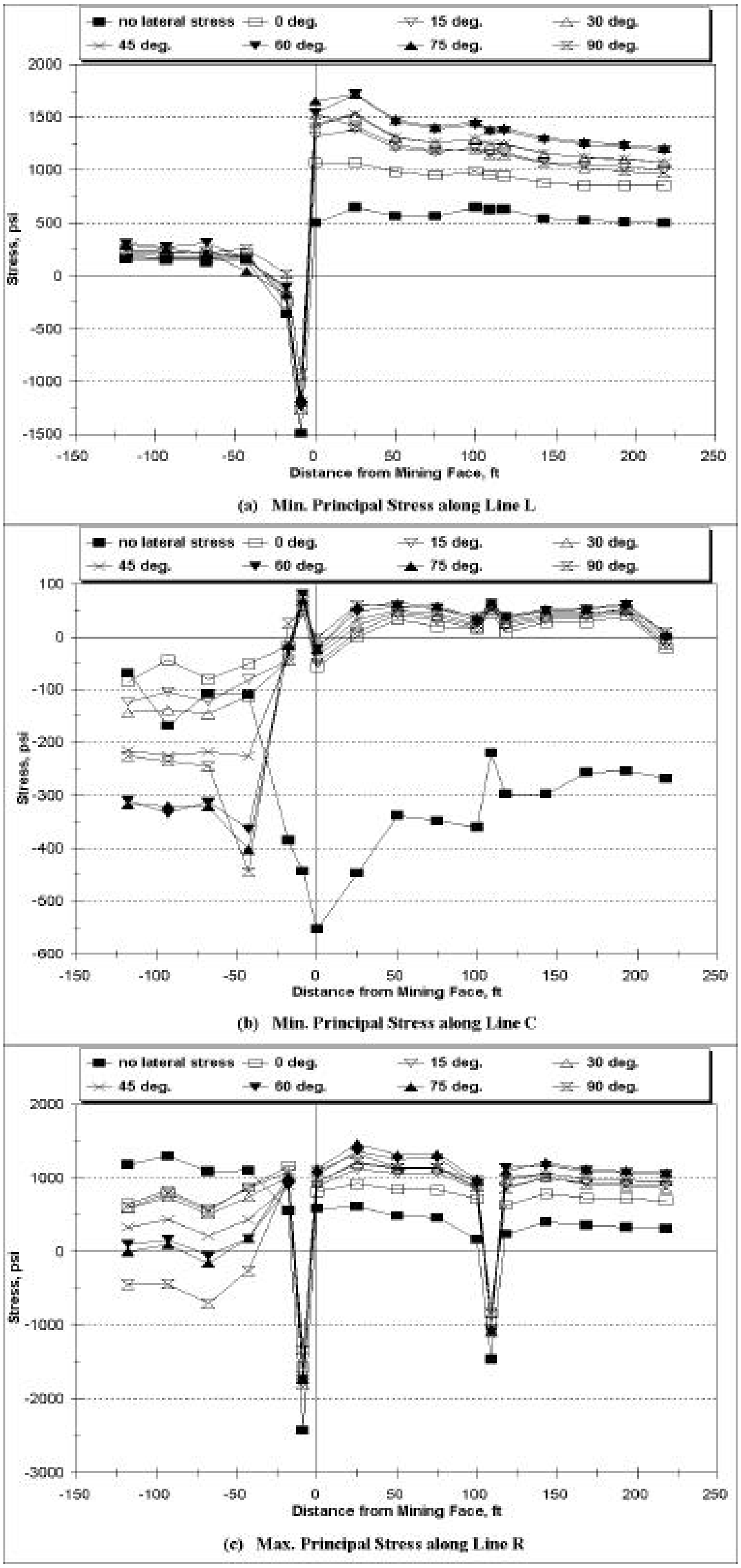

Fig. 5-18 Min. Principal Stress in Tailgate 1 (in single panel)

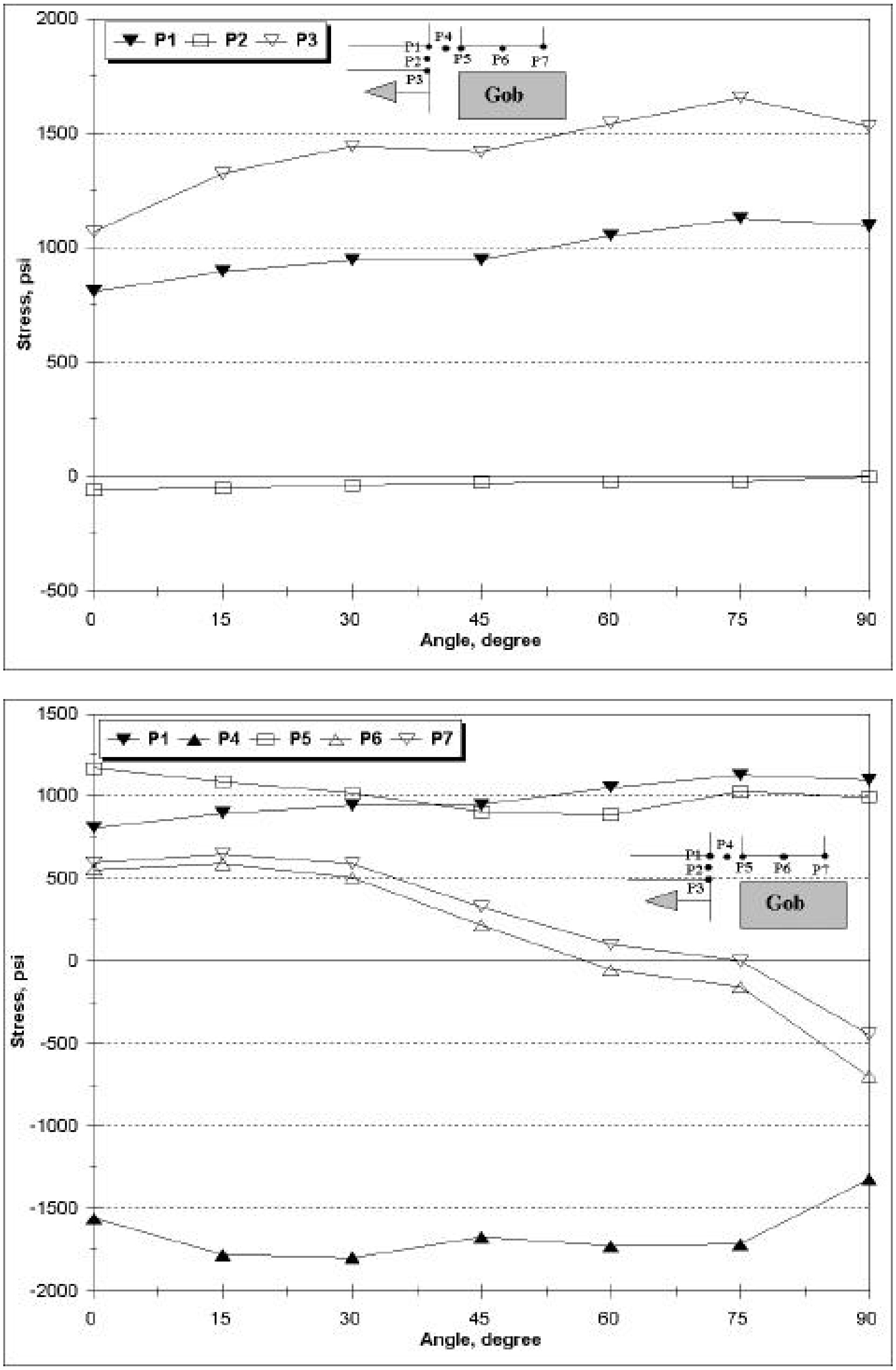

Fig. 5-19 Min. Principal Stress at the Some Points in Tailgate 1 (in single panel)

Comparison of Stresses between Headgate 1 and Tailgate 1

In this study, the maximum horizontal stress is from the headgate side, as shown in Fig. 5-1. Because of the gob effect, the stress at the headgate T-junction is not the same as that at the tailgate T-junction. In the following, the stress differences at the specified points, P1, P3, and P5, are analyzed.

a. Von-Mises Stress

At point P1, the Von-Mises stresses in headgate 1 and tailgate 1 are shown in Fig. 5-20(a). It indicates that the Von-Mises stress in tailgate 1 is less than that in headgate 1 at point P1. At point P3, the stress in tailgate 1 is also less than that in headgate 1 when the angle is equal to or less than 60^0, as shown in Fig. 5-20(b). When the angle is more than 60^0, the difference is very small. However, at point P5, the difference is larger when the angle is not equal to 0^0 or 90^0, as shown in Fig. 5-20(c).

Generally, when the angle is equal to 0^0 or 90^0, the Von-Mises stress at the two T-junctions is the same. When the angle is not equal to 0^0 or 90^0, the Von-Mises stress at the headgate T-junction is larger than that at the tailgate T-junction.

b. Maximum Principal Stress

The maximum principal stress at points P1, P3, and P5 in headgate 1 and tailgate 1 is shown in Fig. 5-20(d)~(f). These figures also indicate that when the angle is equal to 0^0 or 90^0, the maximum principal stress at the two T-junctions is the same, and that when the angle is not equal to 0^0 or 90^0, the maximum principal stress at the headgate T-junction is larger than that at the tailgate T-junction.

Based on the above stress analysis, the stress at the headgate T-junction is larger than that at the tailgate T-junctions when the maximum horizontal stress is from the headgate side. This indicates that the headgate side may have more roof failures in the form of cutter roof than the tailgate in this situation. If the maximum horizontal stress is from the tailgate side, the stress at the tailgate T-junction is larger and the tailgate side may have more roof failures.

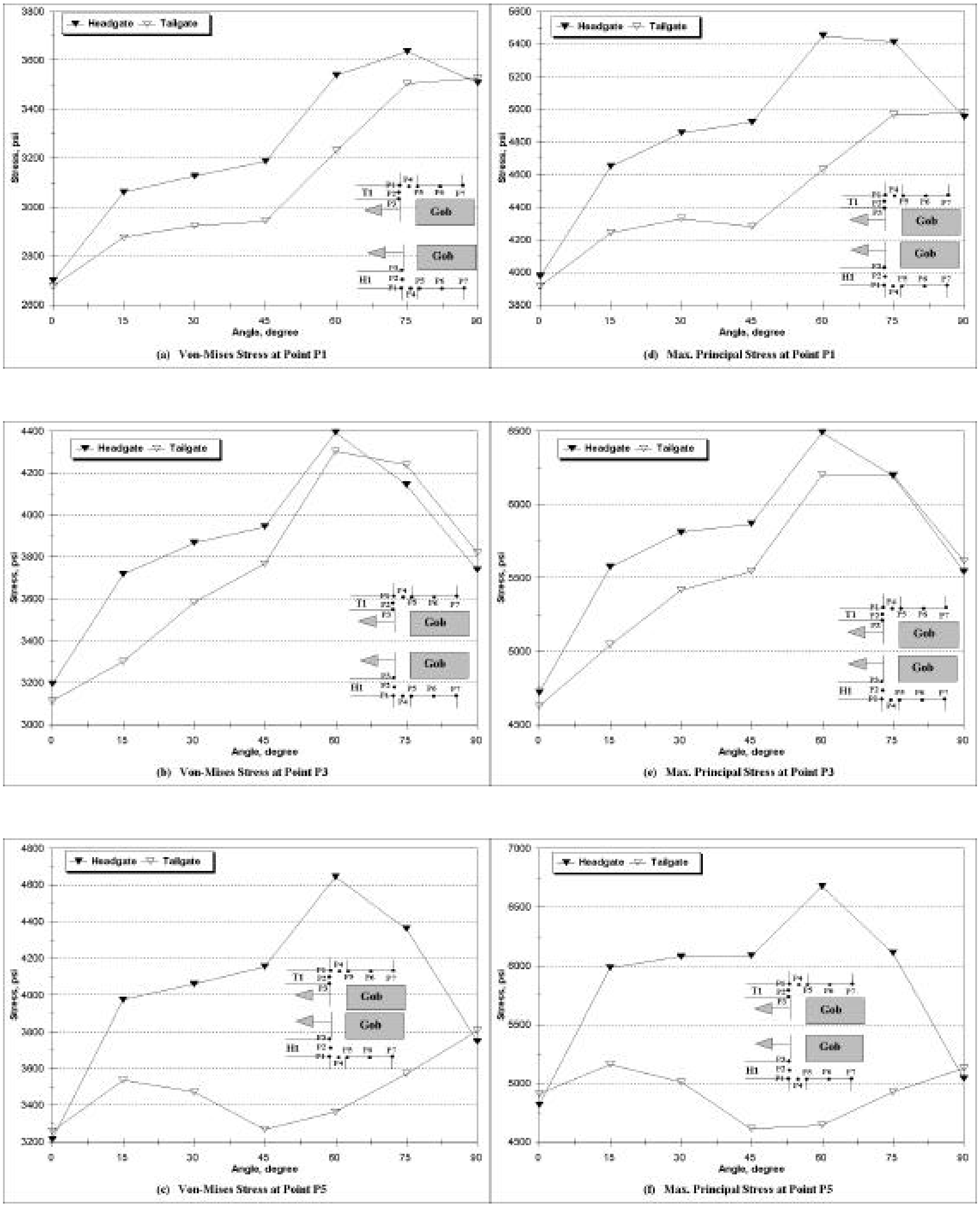

Fig. 5-20 Comparisons of Stresses at the Two T-Junctions (in single panel)

<u>Stress Distributions in Headgate 2 and Tailgate 2</u>

Generally, the stress in the immediate roof of headgate 2 (or tailgate 2) is less than that in headgate 1 (or tailgate 1) in a single panel. Since the angle influence on the minimum principal stress is not significant, the Von-Mises stress and the maximum principal stress in headgate 2 and tailgate 2 are analyzed in the following.

a. Stresses in Headgate 2

The Von-Mises stress at the roof line level of headgate 2 is shown in Fig. 5-21. It indicates that the Von-Mises stress is concentrated at the two rib sides. Along lines L and R, the stress is larger than that along line C. Along line L, the Von-Mises stress increases with the angle between the mining direction and the maximum horizontal stress from 0^0 to 75^0, and then decreases slightly from 75^0 to 90^0. Along line R, the stress increases with the angle from 0^0 to 90^0, except at a few points. At the center (along line C), the stress increases with the angle from 0^0 to 60^0, and then decreases slightly from 60^0 to 90^0.

At the intersection between headgate 2 and the crosscut, the Von-Mises stress is larger. The stress at the intersection is shown in Fig. 5-22. At point P1, the Von-Mises stress increases with the angle from 0^0 to 75^0, and then decreases slightly from 75^0 to 90^0. At point P3, the stress increases with the angle from 0^0 to 60^0, and then decreases from 60^0 to 90^0. When the angle is less than 75^0, the stress at point P3 is larger than that at point P1. At point P4, the Von-Mises stress increases with the angle from 0^0 to 60^0, and then decreases slightly from 60^0 to 90^0. It is found that the Von-Mises stress at points P3 and P4 changes with the angle in the same way. At point P6, the Von-Mises stress increases with the angle from 0^0 to 90^0. At points P2 and P5, the stress changes with the angle, but the angle influence on the stress at these two points is not significant. However, at points P7 and P8, the angle influence on the stress is significant. When the angle is about 15^0, the Von-Mises stress at points P7 and P8 reaches the maximum. When the angle is more than 45^0, the stress is smaller at these two points.

The maximum principal stress in headgate 2 is shown in Fig. 5-23. The maximum principal stress distributions are similar to the Von-Mises stress distributions. The maximum principal stress is concentrated at the two rib sides. The stress increases with the angle from 0^0 to 60^0 or 75^0, and then decreases slightly. At the intersection, the maximum principal stress at points P1~P8 is shown in Fig. 5-24. At the four pillar corners (P1, P3, P4, P6), the stress increases with the angle. When the angle is about $60^0 \sim 75^0$, the stress at point P4 is the maximum.

Based on the above stress analysis, it is found that headgate 2 is in the worst condition when the angle is about $60^0 \sim 75^0$.

b. Stresses in Tailgate 2

The Von-Mises stress at the roof line level in tailgate 2 is shown in Fig. 5-25. The stress is concentrated at the rib sides. Along line L, the stress increases with the angle from $0^0 \sim 90^0$. The Von-Mises stress is large in the range of -100 ~ 100 ft. Along the other rib side (line R), the Von-Mises stress increases with the angle from $0^0 \sim 90^0$, except at pillar corners. It is also large in the range of -100 ~ 100 ft. At the center of the entry (line C), the Von-Mises stress increases slightly with the angle from $0^0 \sim 90^0$.

At the intersection between tailgate 2 and the crosscut, the Von-Mises stress at the specified points is shown in Fig. 5-26. The stress at point P1 increases with the angle from $0^0 \sim 60^0$, and then decreases slightly from $60^0 \sim 90^0$. But at point P3 (a pillar corner), the stress increases with the angle from $15^0 \sim 90^0$. At point P4, the stress changes with the angle in the same way as that at point P3 except when the stress angle is less than 15^0. When the angle is about 90^0, the Von-Mises stress at point P4 reaches the maximum. At point P6, the stress changes with the angle in the same way as that at point P1, namely, the Von-Mises stress increases with the angle from $0^0 \sim 60^0$, and then decreases from $60^0 \sim 90^0$. At points P2 and P5, the Von-Mises stress changes with the angle. But the angle influence on the stress at these two points is not significant. At points P7 and P8, the Von-Mises stress increases with the angle from $0^0 \sim 15^0$, and then decreases from $15^0 \sim 90^0$. When the angle is about 15^0, the Von-Mises stress at points P7 and P8 is the maximum.

The maximum principal stress at the roof line level in tailgate 2 is shown in Fig. 5-27. The stress is concentrated at the rib sides. Along line L, the maximum principal stress reaches the maximum when the angle is about $60^0 \sim 75^0$. At the range of –100 ~ 0 ft inby the face, the stress is larger than that in the range of 0 ~ 100 ft. Along line R, the maximum principal stress increases with the angle from $0^0 \sim 60^0$, and then decreases slightly from $60^0 \sim 90^0$.

At the intersection between tailgate 2 and the crosscut, the maximum principal stress at the points, numbered P1 ~ P8, is shown in Fig. 5-28. It indicates that the stress at points P1 and P6 increases with the angle from $0^0 \sim 60^0$, and then decreases slightly from $60^0 \sim 90^0$. At points P3 and P4, the stress increases with the angle from $0^0 \sim 90^0$. At the center points P2, P5, P7, and P8, the angle influence on the maximum principal stress is smaller.

Generally, tailgate 2 will be in the worst condition when the angle is about $60^0 \sim 75^0$ based on the above stress analysis.

<u>Comparison of Stresses between Headgate 2 and Tailgate 2</u>

Because of the gob effects, the Von-Mises stress and the maximum principal stress in headgate 2 are not the same as those in tailgate 2. They are compared at some specified points, at which the stresses can stand for the stress situations in the entries. The specified points are shown in Fig. 5-29, numbered P1 ~ P12. As analyzed in the previous section, the maximum principal stress distributions are similar to the Von-Mises stress distributions, as shown in Fig. 5-20. Therefore, only the Von-Mises stress is compared at those points in headgate 2 and tailgate 2.

At point P1, the Von-Mises stress in headgate 2 and tailgate 2 is shown in Fig. 5-29(a). That the Von-Mises stress in headgate 2 is less than that in tailgate 2. At points P3 and P4, the Von-Mises stress in headgate 2 is larger than that in tailgate 2, as shown in Fig. 5-29(b) and (c). At point P6, where the stress distributions are similar to those at point P1, the Von-Mises stress in headgate 2 is less than that in tailgate 2.

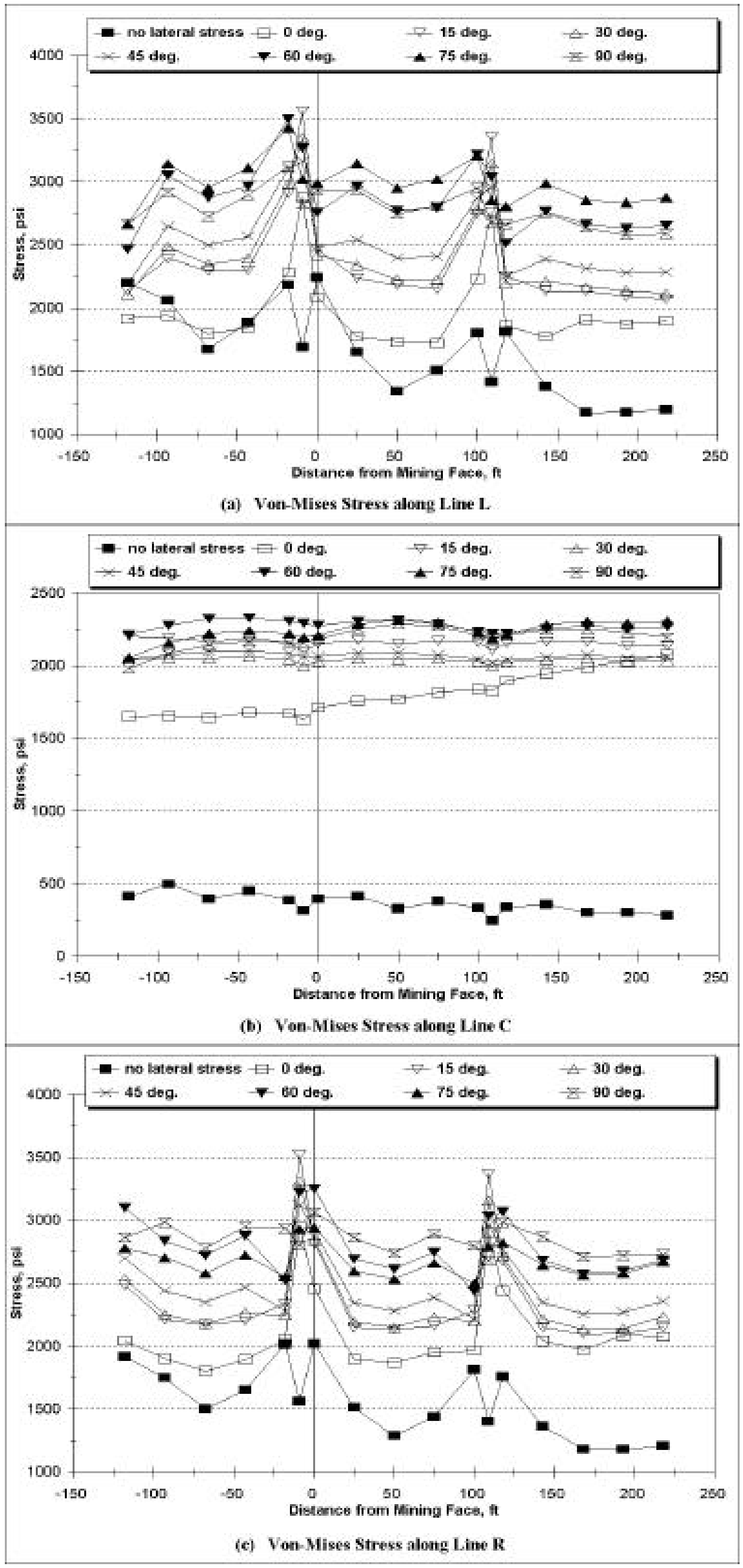

Fig. 5-21 Von-Mises Stress in Headgate 2 (single panel)

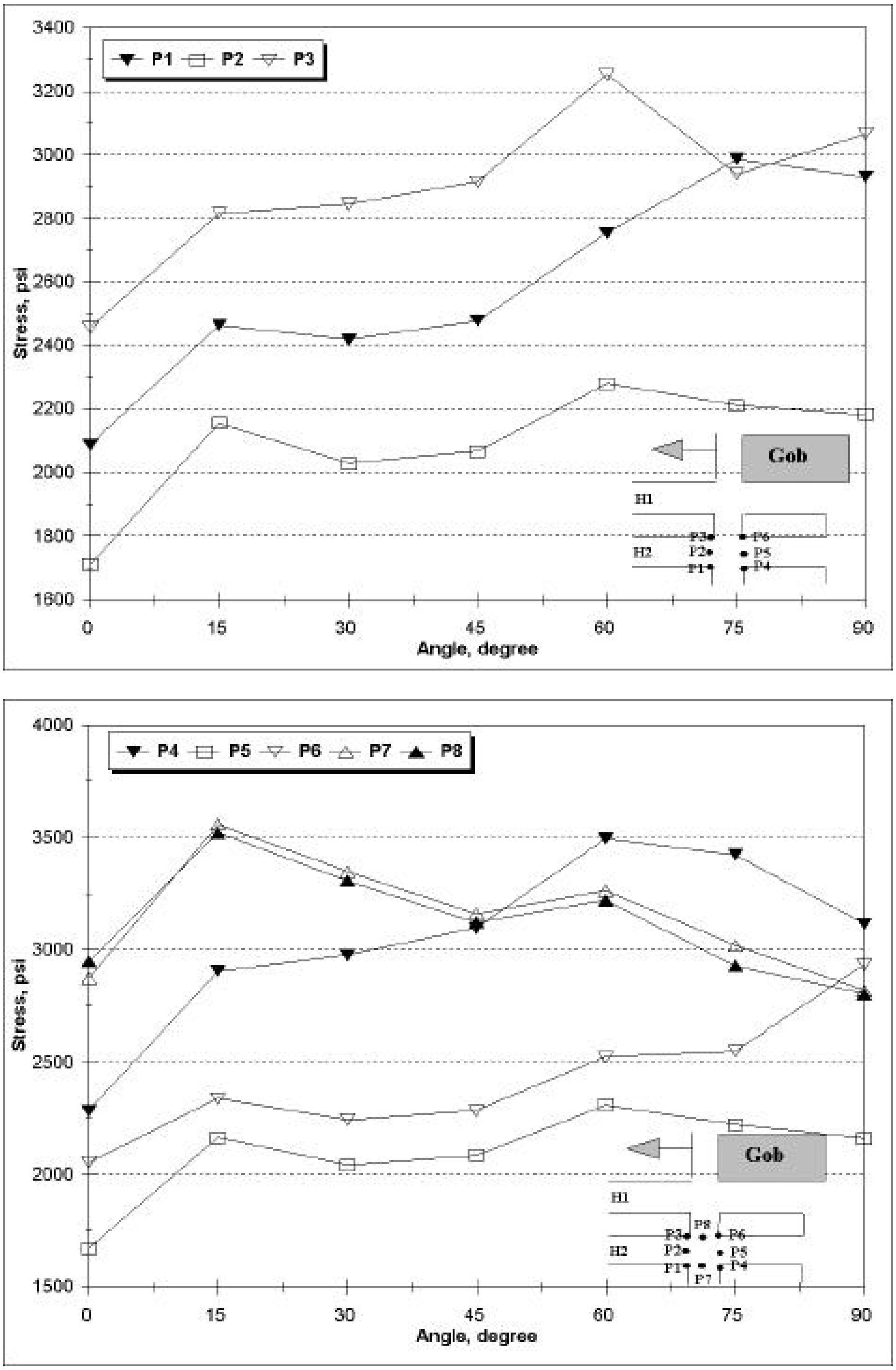

Fig. 5-22 Von-Mises Stress at the Specified Points in Headgate 2 (single panel)

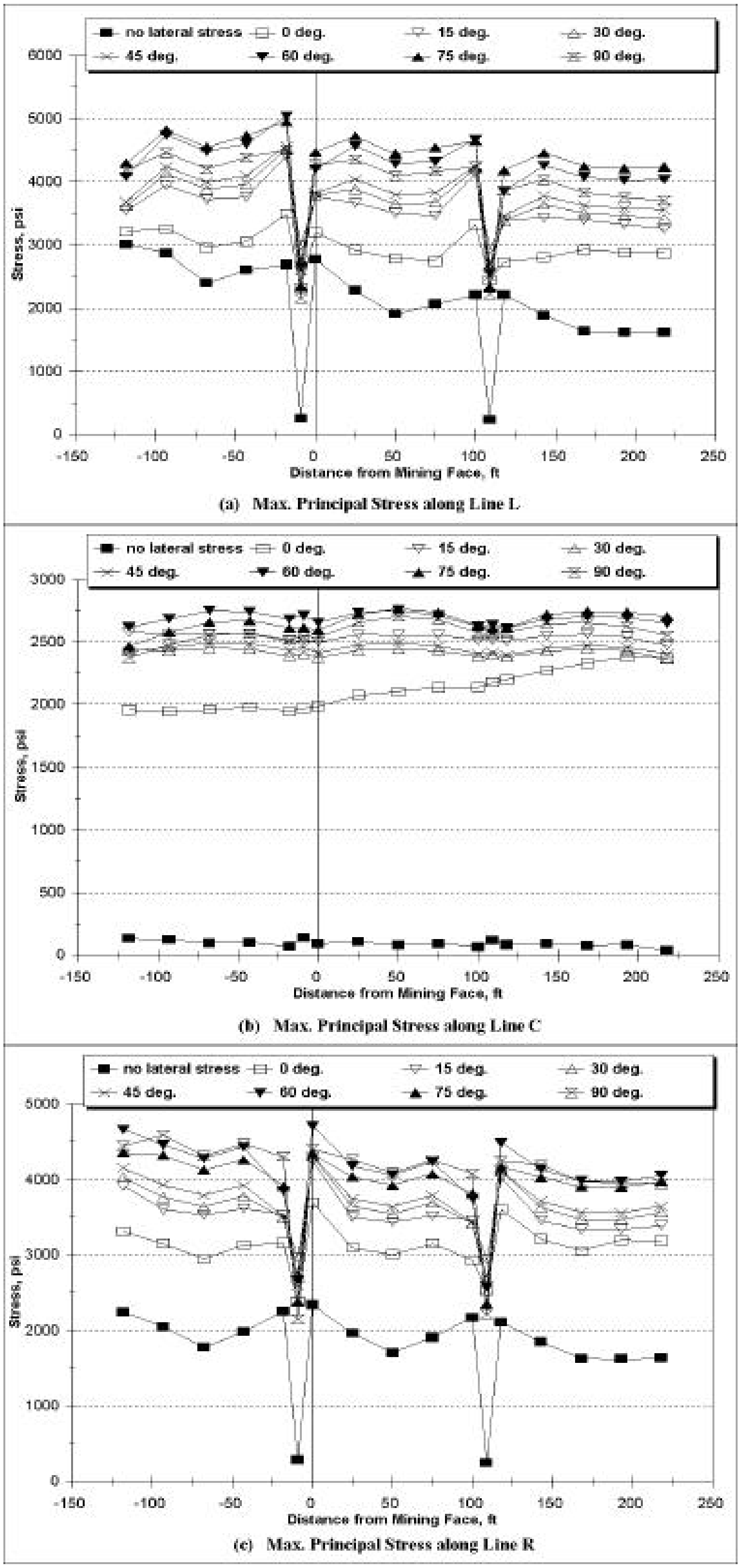

Fig. 5-23 Max. Principal Stress in Headgate 2 (single panel)

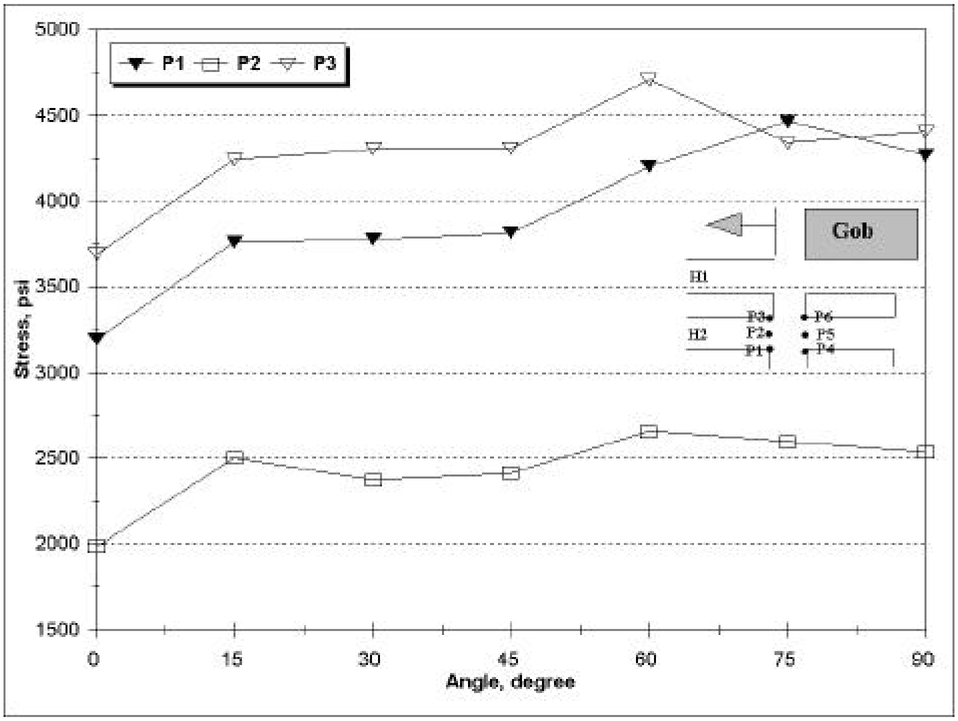

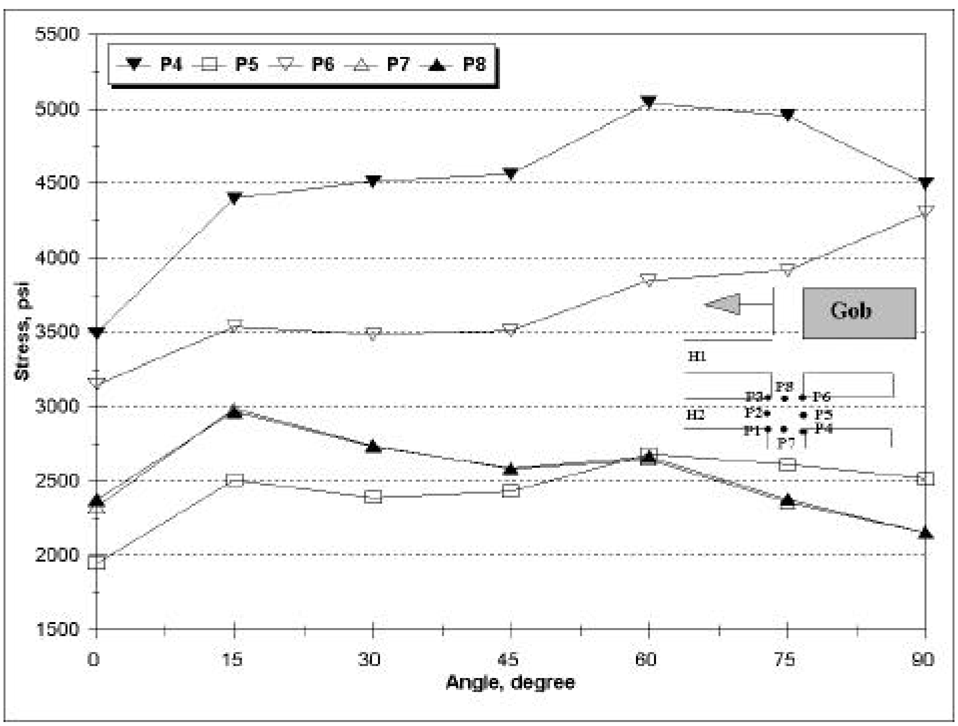

Fig. 5-24 Max. Principal Stress at the Specified Points in Headgate 2 (single panel)

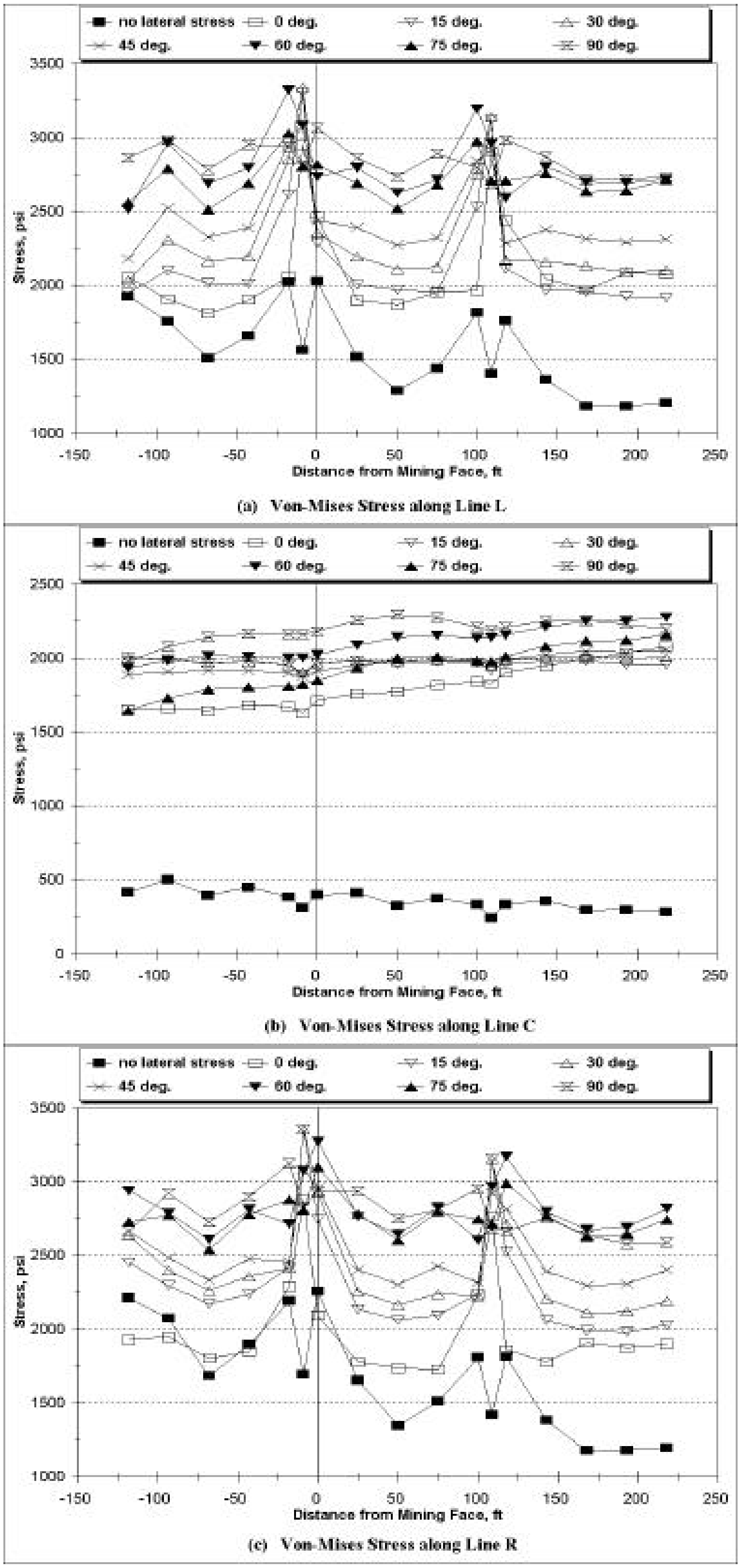

Fig. 5-25 Von-Mises Stress in Tailgate 2 (single panel)

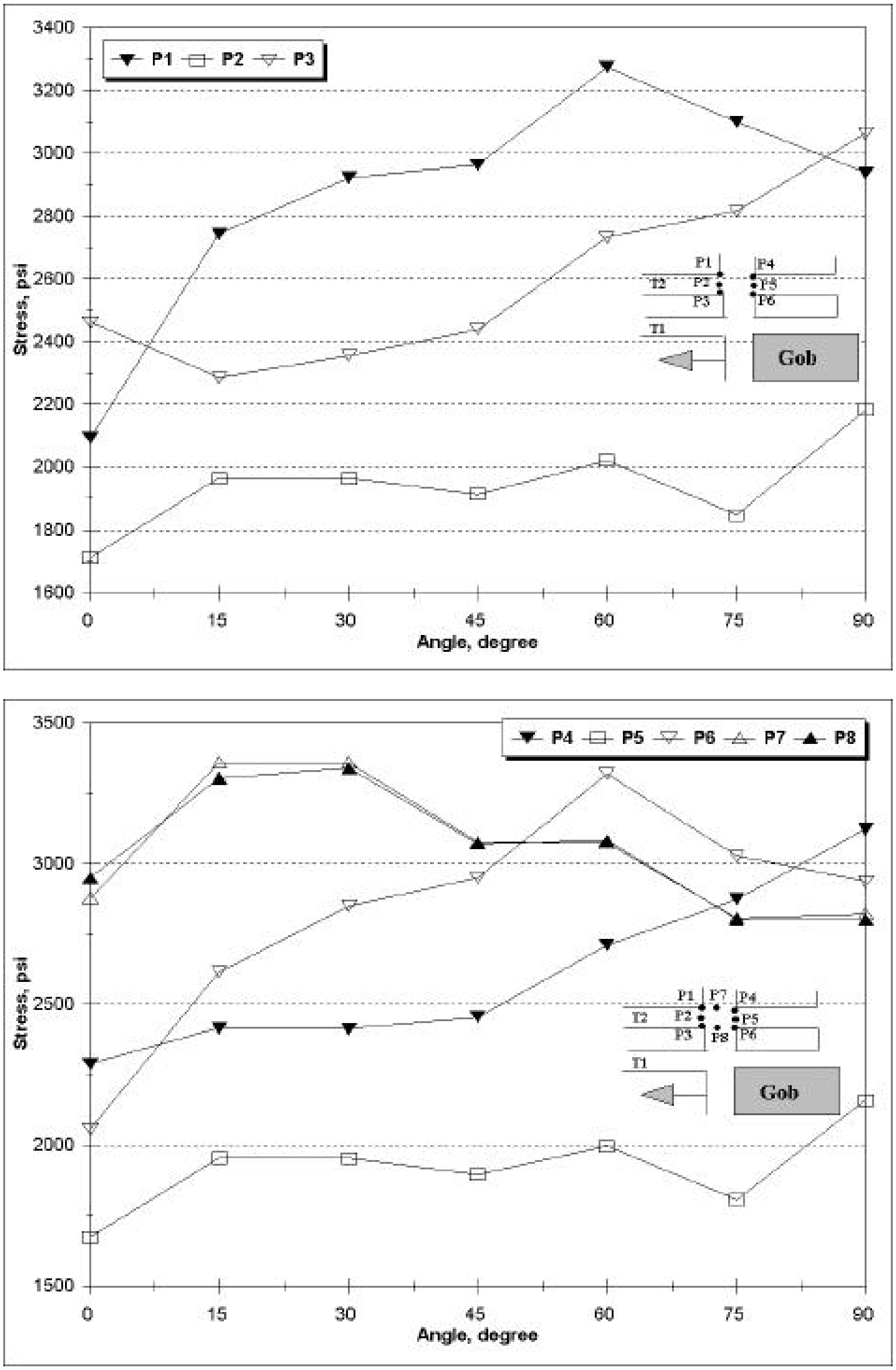

Fig. 5-26 Von-Mises Stress at the Specified Points in Tailgate 2 (single panel)

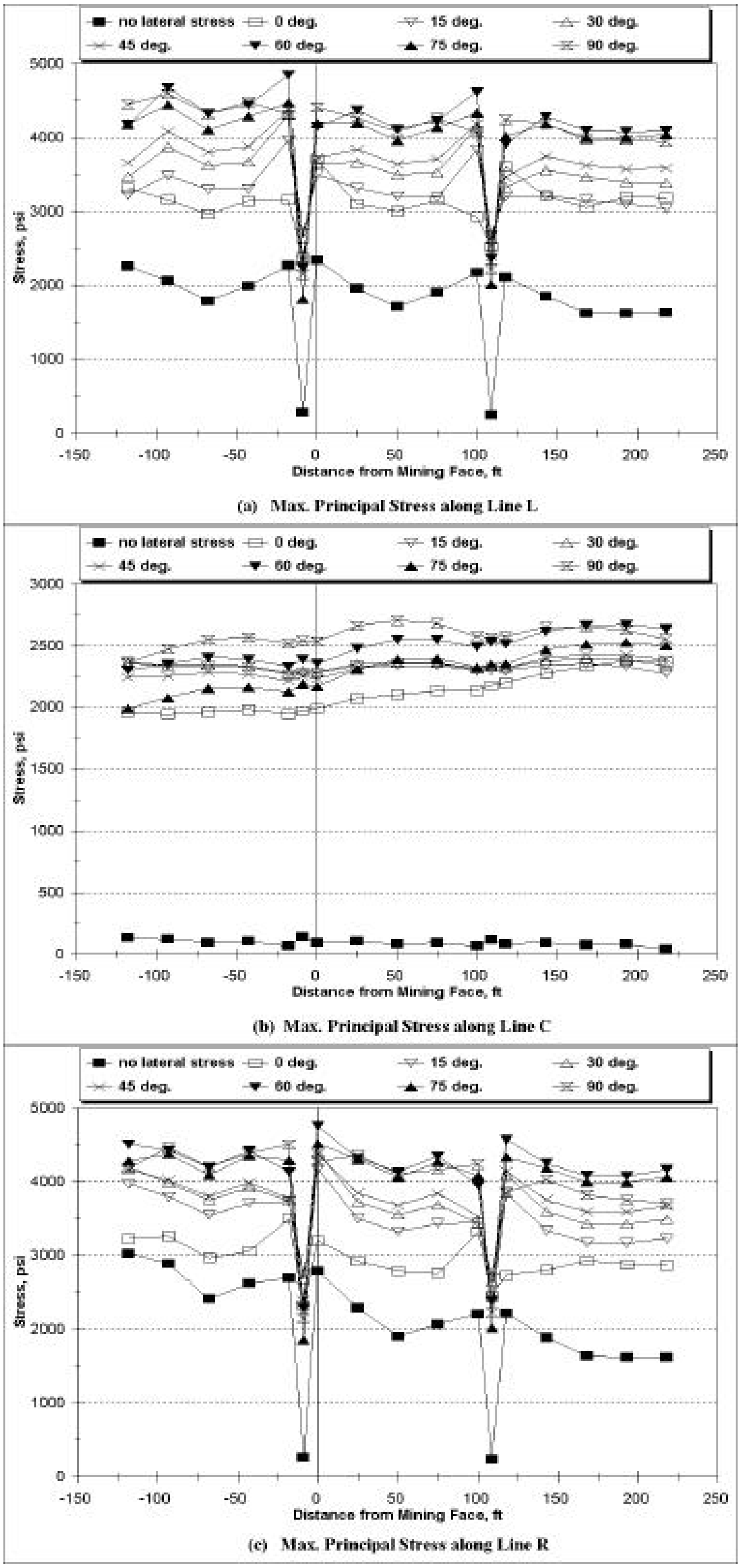

Fig. 5-27 Max. Principal Stress in Tailgate 2 (single panel)

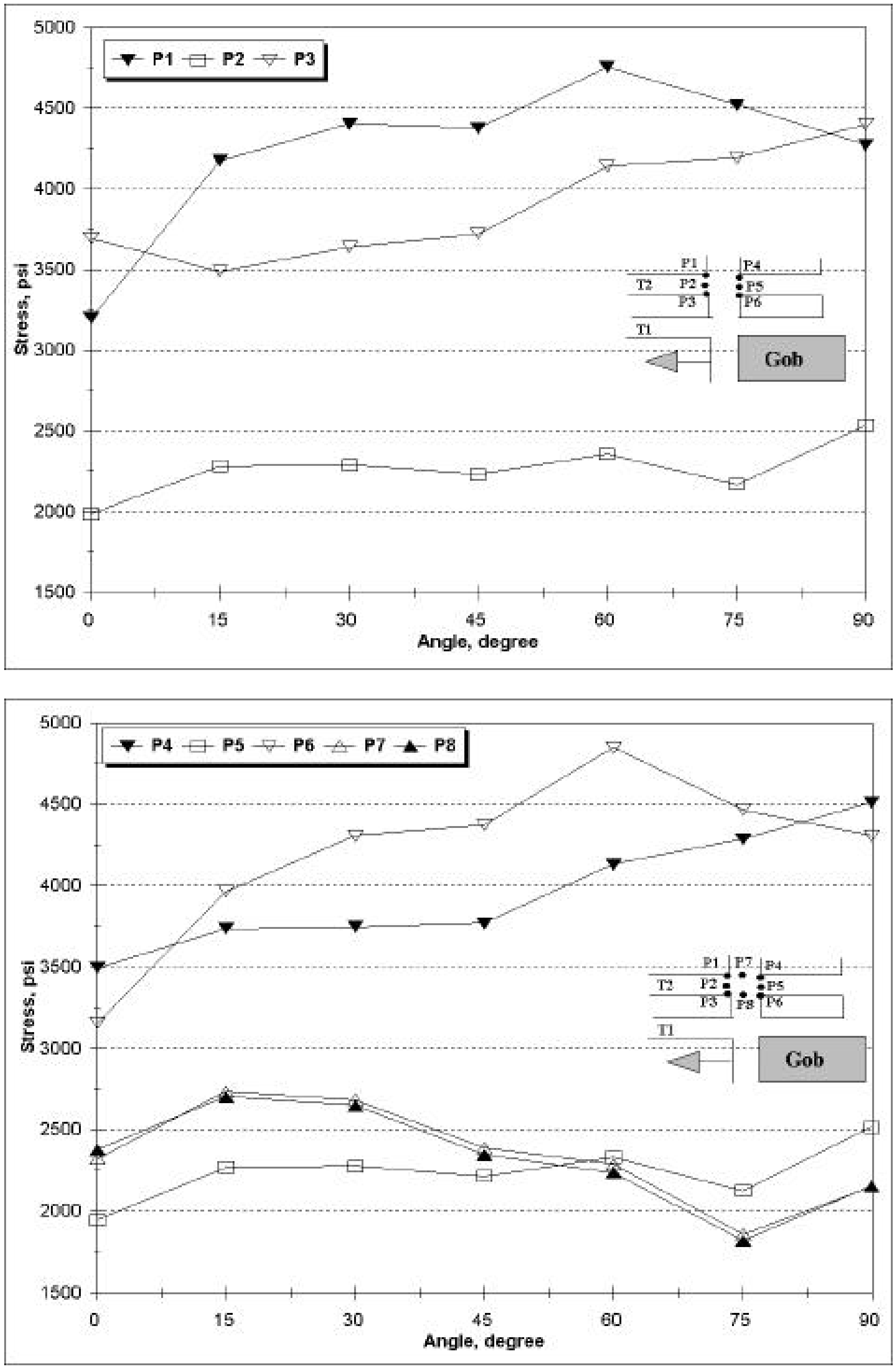

Fig. 5-28 Max. Principal Stress at the Specified Points in Tailgate 2

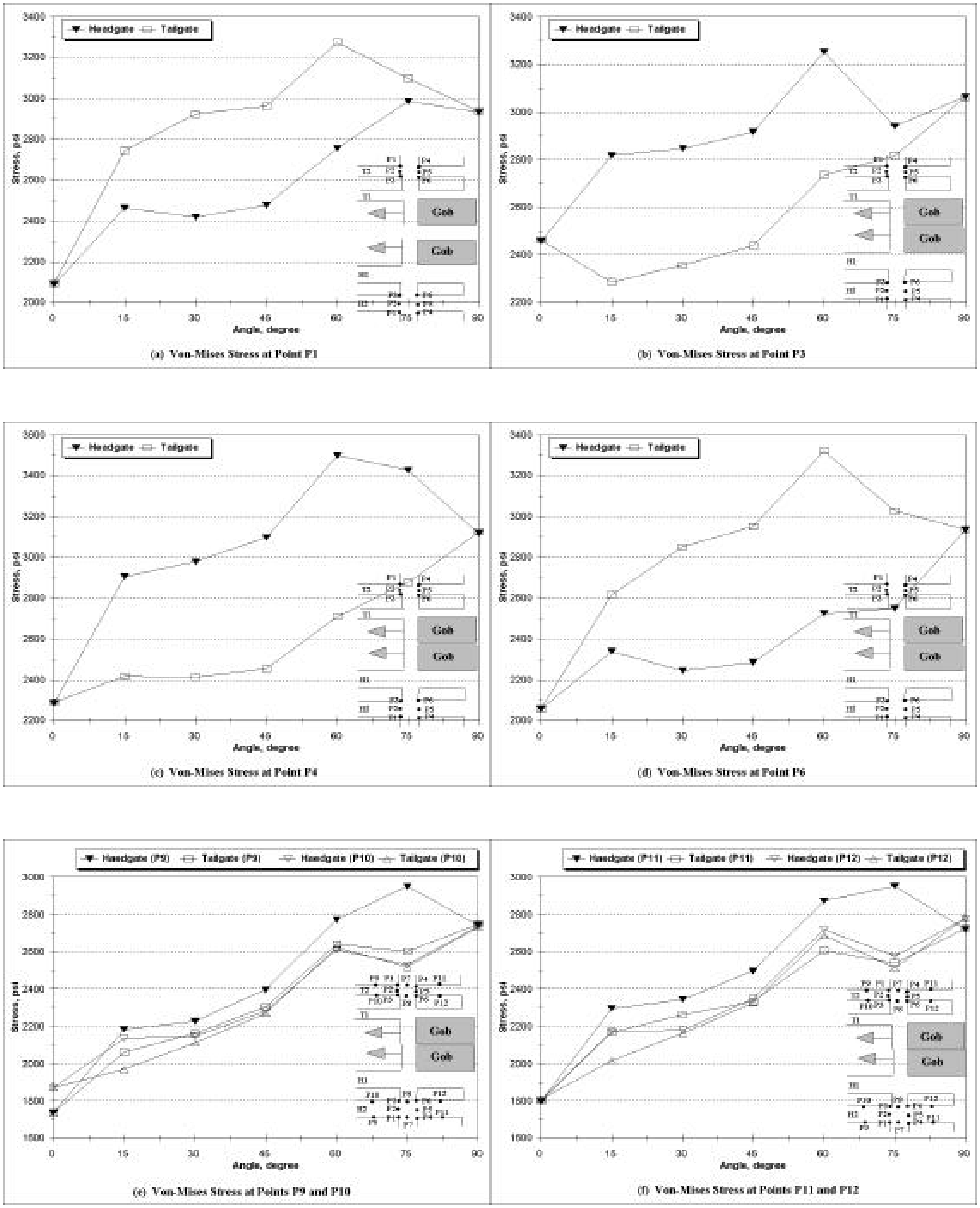

Fig. 5-29 Comparisons of Von-Mises Stress at the Specified Points in Headgate 2 and Tailgate 2